Mathematical Analysis and Its Application to Kassa Basaltic Rocks of Jos Plateau State, Nigeria

Lekmang C. Isah[1], Hyeladi Dibal[2], Achuenu Ifeanyi[3]

[1]Department of Geology, University of Jos Plateau State, Nigeria

[2]Department of Geology, University of Jos, Plateau State, Nigeria

[3]Department of Mining Engineering, University of Jos Plateau State, Nigeria

Abstract

Mathematically, the formation of rock forming minerals from magma, depends on the numerical values of each mineral under thermodynamic conditions. This research was focused on application of mathematical equations using Bowen's and Goldschmidt concepts to calculate the numerical values of minerals in Kassa Basaltic rocks of Jos Plateau state, Nigeria. Findings have shown that, under mathematical context, Bowen's and Goldschmidt rules were mathematically connected. Under mathematical context, it is was concluded that the examinations of sampled rocks collected from Kassa Volcanic Basalts, under thin section and chemical analysis using ICPMS, indicate, that minerals observed and chemical composition analyzed, fall within gabbro clan. The gabbro clan includes basalt, dolerite, norite, scoria and gabbro and therefore under mathematically context, Kassa volcanic Basalts particularly for KIA1, are characteristics of rocks of Gabbro clan and the rock type for KIA1 is olivine, alkali basalt magma type. Finally the "mathematical connection" between Bowen's and Goldschmidt concepts was used in this research for a concise explanation of rock forming minerals from the beginning to the end of crystallization and would help the 'beginners' especially students of Earth sciences such as Geology, Mineralogy, Petrology and other chemical sciences such as Chemistry, Geochemistry and Petroleum Geology to have clear understanding of rock forming minerals from the Resident magma ($\mathfrak{R}$).

Keywords

Mathematical Analysis, Minerals, Rocks, Magma

1. Introdiction

Application of mathematics to some aspect of sciences, such as physics, chemistry and other engineering disciplines has been successful over the years and several inventions have been made to solve scientific and engineering problems to enhance human comfort, but in the case of geology application of mathematics is not that much satisfactory and this research emphasizes on challenge arises using mathematical framework concerning the "problem of elemental substitution and distribution of chemical elements in igneous rocks throughout the time of crystallization from the beginning to the end of crystallization with mathematical foundation under thermodynamic change

The gap between Bowen's and Goldschmidt concepts concerning the problem of elemental substitution and distribution of chemical elements in rocks throughout the time of crystallization from the beginning to the end of crystallization would be investigated using mathematical context with respect to thermodynamic principles.

Application of mathematics to some aspect of sciences, such as physics, chemistry and other engineering disciplines has been successful over the years and several inventions have been made to solve scientific and engineering problems to enhance human comfort, but in the case of geology application of mathematics is not that much satisfactory and this research emphasizes on challenge arises using mathematical framework concerning the "problem of elemental substitution and distribution of chemical elements in igneous rocks throughout the time of crystallization from the beginning to the end of crystallization with mathematical foundation under thermodynamic change according to Achuenu. This research focuses on application of mathematical equations to Kassa Basaltic rocks of Jos Plateau state, Nigeria in connection with Bowen's and Goldschmidt concepts.

The gap between Bowen's and Goldschmidt concepts concerning the problem of elemental substitution and distribution of chemical elements in rocks throughout the time of crystallization from the beginning to the end of crystallization was investigated using mathematical context with respect to thermodynamic principles according Achuenu and others [1].

Geometrically, several minerals set in matrices and aggregate themselves in coordinate to form rocks and chemical elements of several properties bonded together to form minerals, which by definition is inorganically in composition with distinct chemical composition. Goldschmidt classified these elements according to their class of materials such as siderophile, lithophile and chalcophile elements as well as atmophile elements [2]. But Mendeleev's arranged these elements in periodic table according to size and atomic mass. According to modern periodic law, atomic number increases from left to right and from top to bottom of periodic table. Therefore the size and electronegativity of elements increase across the period and the size increases with decreasing electronegativity down the group. This pattern of modern periodic law would be used to explain how ions would enter into the lattice of a growing crystal during crystallization of silicate magma as a function of size and electronegativity. During crystallization of magma, temperature falls, with increasing content of silicon in the magma. This forms two series of reactions (Bowen's), one by interaction with magma, with the first mineral formed, to form minerals of different chemical composition, but with the same crystallographic structure. This is the case of solid solution in the magma. While the other, the first crystal to form, initially interact with the magma to form a solid with different crystallographic structure, and distinct chemical composition. This is the case of fractional crystallization in the magma.

The term solid solution and fractional crystallization are used simultaneously in this research to define the two series of reactions as stipulated by Bowen's reaction series.

Mathematically, the formation of rock forming minerals from magma $\mathfrak{R}$, depends on the numerical values of each of the minerals under thermodynamic change. Any stable materials depend on the numerical values for those materials to exist at that certain ambient temperature, especially at room temperature of 25^0C (298k), at 1atm pressure. The problem involving the distribution of chemical elements and elemental substitutions in rock during crystallization of magma $\mathfrak{M}$ from the beginning of crystallization to the end of crystallization would be postulated to some an extent using combined Goldschmidt and Bowen's concept with respect to electronegativity and radius ratio, which states that, for ions of various electronegativities and sizes to compete for the space in a lattice of a growing crystal [3].

1. The one with more electronegative would preferentially enter into the lattice of the growing crystal of silicate radical because the nucleus of silicate radical is electronegative provided modern periodic law is obeyed and
2. That ions of closest radius (δ) to the nucleus of formed crystal substitute themselves before the ion of other radius ratio according to Wood.

Both olivine and pyroxene are silicates that contain a variable amount of magnesium (Mg^{2+}) and iron (Fe^{2+}). Pure magnesium olivine that does not contain iron is forsterite. The other end member of the olivine series with iron instead of magnesium is called fayalite. Chemicalexpressions for olivine are $(Mg, Fe)_2$ SiO_4 or SiO_4 where denotes the fraction of Mg atoms in olivine. The variable then is equivalent to our variable which is measured in percent. When $x_0=1(or\, y_1=100)$, the formula becomes Mg_2 SiO_4 for forsterite. Orthopyroxene has chemical composition SiO_3. When $x_p=1(y_2=100)$, we have the end member enstatite: when $x_p=0$, the pyroxene is called ferrosilite. In a system where olivine and pyroxene coexist, a chemical process may take place in that some Fe^{2+} ions go from olivine to pyroxene or vice versa. Simultaneously, the same quantity of Mg^{2+} ions goes in the opposite direction.

2. Literature Review

2.1 Introduction

Krumbein and Grayhill have distinguished three types of models in geology: (1) scale-models: (2) conceptual models: and (3) mathematical models. Traditionally, geologists have been concerned with scale-models and conceptual models mainly.

Examples of scale-models are the geological map and cross-sections where the spatial variability of attributes is represented at a reduced scale for topographic surface and vertical planes, respectively. Geological processes also can be represented by scale-models. Conceptual models are mental images of variables and constants. They are statistical or deterministic depending on whether one or more random variables are used in the equation or systems of equations to express uncertainty. Mathematical equations generally can be represented geometrically by curves or surfaces.

The three types of models listed are not mutually exclusive. Scale-models can be based on mathematical criteria and conceptual models may be partly or entirely quantitative. Most mathematical models in geology have some important aspects of uncertainty and for this reason, are statistical. The problem may consist of eliminating the random variations from data so that a deterministic expression is retained representing the relationship between averages for assemblages of attribute rather than between single features. Statistical components or the uncertainty provide a way of expressing a range of different extrapolations for single features, all of which are possible, but with different probabilities of occurrence. This method replaces that of extrapolating a phenomenon with absolute certainty.

Geology differs from physics, chemistry and other sciences in that the possibility of doing controlled experiment is more limited. The observations are restricted to a record of past events, making geology a historical science. Generally, the final product of many interrelated processes is exposed at the surface of the earth in an imperfect manner. These mainly physical-chemical processes seldom reached a state of equilibrium: most came to a halt before reaching equilibrium at one or more specific points of time.

Basalts mainly consist of two minerals: plagioclase and pyroxene. Barth discussed the following simplified model [4]. Basalt magma can be defined as a silicate melt that on cooling yields plagioclase and the pyroxene. These may be considered in terms of two main reaction series: (1) the series of plagioclase fledspars going from calcic to sodic composition (Ca→Na): and (2) a series of clinopyroxenes developing from diopside to hypersthenes (Mg→Fe). Although this is an oversimplification of pyroxene cyrstalisation relationships, it will be helpful for our discussion to use this combination of the two processes for representing the principal crystallization process of basaltic magma. At specific compositions of magma, the second series can begin with initial precipitation of olivine that, on further cooling is converted into pyroxene.

The relationship between the two processes is shown graphically in Fig (1), below. There is a boundary OP in the center of this illustration. If the composition of the original basaltic liquid lies to the right of OP, crystallization will start precipitation of only pyroxene. If it is located to the left of the boundary, only plagioclase will be formed. Because of the precipitation of crystals, the magma composition will change describing a path that is directed to the center. Once the line OP is reached, simultaneous precipitation of both mineral phases takes place. A melt of composition O crystallizes by simultaneous formation of pyroxene of composition A and plagioclase of composition Q. As crystalisation proceeds, the melt changes from O to P and the two solid phases change from A to B and from Q to R. Figure 1 beolw is only approximate and the model which has four constituents cannot be completely represented by it. For a more complex representation, a tetrahedron with four corner points can be used for projection (cf. Barth,. One of the objectives of a model of this type is to classify a given basaltic rock. After the mode of the norm has been calculated for a basalt sample, the result can be projected on a phase diagram and from the position of the point with respect to one or more boundaries such as OP in Fig.2, it can be conducted which solid phase has crystallized first: plagioclase or pyroxene.

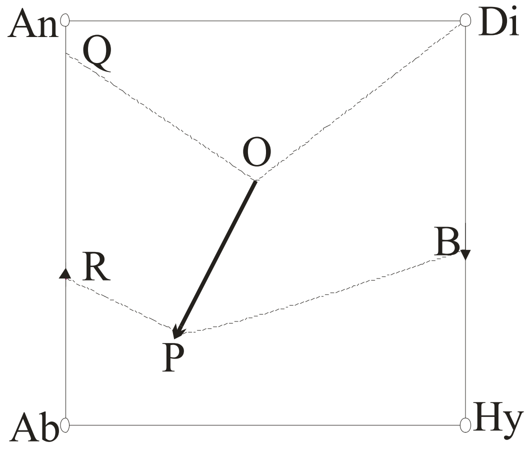

Figure 1. Schematic Presentation of the Crystallization process of Basaltic lavas

Source: From Barth (1962)

Another practical application is as follows. Suppose that basaltic magma occurs in an underground magma chamber which is subject to cooling and where continuous precipitation of crystals takes place in the manner described above. Suppose further that periodically some magma escapes from the chamber to the surface of the earth where it forms basalt lavas. An assemblage of samples from these lavas may show some regularities in the relationship between components. Ca-rich plagioclase will tend to coexist with Mg-rich pyroxene. If the major oxides for a suite of basalts are correlated to one another, regardless of time deposition, the following signs may occur for the coefficients in the correlation matrix as presented in table 1.

Table 1. Coefficient of Correlation Matrix

	FeO	MgO	CaO	Na_2O
FeO	1			
MgO	-	1		
CaO	-	+	1	
Na_2O	+	-	-	1

Sourse: From Barth (1962).

Likewise, if the major oxides are plotted against time, the cooling of an underground magma chamber may be reflected at the surface where and decrease whereas and Na_2O increase with time. In this example, the time of deposition can be entered as a variable by sampling successive flows in a volcanic pile from bottom to top.

Bowen’s reaction principle a concept, first propounded in 1928 by Norman Bowen, which explains how mineral can respond to changing equilibrium conditions when a magma is cooled, by either a continuous diffusing – controlled exchange of elements with the magma or discontinuous melting of the material.

The periodic law was developed independently by Dmitri Mendeleev and Lothar Meyer in 1869 [5]. Mendeleev created the first periodic table and was shortly followed by Meyer. They both arranged the elements by their mass and proposed that certain properties periodically reoccur. Meyer formed his periodic law based on the atomic volume or molar volume, which is the atomic mass divided by the density in solid form. Mendeleev's table is noteworthy because it exhibits mostly accurate values for atomic mass and it also contains blank spaces for unknown elements.

Goldschmidt proposed his Classical general rules to explain the distribution of the elements, in which ions of similar size and charge substitute themselves.

Ringwood proposed the complementary use of the concept of electronegativity in order to understand the distributions of the chemical elements that could not be explained completely with the Goldschmidtian rules, especially when the minerals being investigated had high percentages of covalent bonding [6].

Nickold proposed that the tree principal factors (ionic size, Ionics charge and electronegativity) be expressed in a single function that would not result in the dichotomous predictions [7].

Bernard J. Wood Modifies Goldschmidt rules 2 and 3, that the site has a preferred radius of Ion (r) which eaters mostly easily, for ions of the same charge, those which are closest in radius to enter most easily, ions whi ch are larger or smaller are discriminated against.

Fournier and Rowe, state that silica Geothermomenter works because that solubility of the various silica minerals (Quartz, and chalcedony, S_iO_2) increase monotonically with temperature [8].

White state Na – K Geothermometer takes advantage of the fact that the equilibrium points of certain exchange reactions among various minerals, principally, the feldspar vary with temperature [9].

Spatial thinking is essential to all spatially dependent sciences, including geography. It comprises the spatial abilities of visualization, orientation and, likely also relation, although contested.

Toramaru, A., and Kichise, T., (2023)**,** proposed a new numerical experiments to study the influence of different cooling rates and classical nucleation theory parameters on the crystal number density measured under constrained conditions in the laboratory experiments [10].

2.2 Origin and Classification of Basalt

Geologists have applied different names to different types of basalts for many years. One of the first major efforts was the distinction between the olivine (and alkali olivine) basalts, which yield an alkaline differentiation sequence, and tholeiites, which yield subalkaline trend, Kennedy and Yoder applied the concept of separate alkali and sub alkali primary basalts which was explored in depth. Green and Ringwood also applied this principle then further clarified the concept of basalts transitional between alkali and tholeiitic. MacDonald and Katsura proposed chemical distinction, rather than normative between alkali basalts and tholeiites. This classification was later challenged by McBirney and Williams. A summary of various chemical characteristics of alkali olivine basalts was given by Schwarzer and Roger [11].

Kuno introduced the term high alumina basalt, in addition to alkali and tholeiitic basalts as potential primary magma. This concept was also discussed by Kushiro and Kuno [12]. The term tholeiite has been modified in various ways. For example, Jakes and Gill distinguished tholeiites of mid-ocean ridges from the early island-arc tholeiite. Miyashiro, etal, [13], discussed compositional variability of the mid-oceani ridge and described high-alumina varieties.

One of the earliest, still used, classification of igneous sequences was given by Peacock. Peacock defined various terms, including calc-alkalic, which has been written as calcalkaline and calc-alkali. Kuno, for example, originally identified pigeonite and hypersthenic series in Japan, he later re-classified these as tholeiitic and calcalkaline respectively [14]. Kuno's critical iron enrichment line, separated tholeiitic (iron-enriched) from calcalkaline (not iron-rich enriched) suites on aluminum, iron, magnesium diagram reproduced from Schwarzer and Rogers. In recent years shoshonite and komatite were recognized. Shoshonites were originally described by Iddings as porphyritic rocks with a set of characteristics more recently summarized by Nicholls and Carmichael. Joplin adopted the term for certain High-K rocks. Her paper also distinguished among High-K shoshonites, high members of alkali basalt suites, and High-Na members of alkali basalt.

2.3 Volcanic Rocks in Jos Plateau

MacKay et.al, termed the Younger Cenozoic volcanic rocks of this area the Newer Basalt, but they divided them into" earlier group" and a "more recent group". McLeod et.al, adopted similar plan, but used different terminology, which is the one used here. Flows and flow remnants lacking a well-defined volcanic focus were termed Older Basalt, as distinct from the typically large valley-filling flows which can be traced to recognizable cones, the Newer Basalts [15].

Older Basalts are generally small, boundary remnants, most of which are demonstrably younger than the fluvio-volcanic series for the rest on erosion surface cut into the laterite, quite fresh. According to McLeod et.al, are dome like outcrops, especially in the southeast which may represent volcanic foci,. They are all basaltic, except for the remarkable "trachyte of Umat Hill near Bukkos, so far the only Cenozoic salic rock known on the plateau.

Newer Basalts as defined by McLeod et.al, cover some hundreds of square Km and extend to southwest of the Jos Plateau. They are mainly made of basaltic scoria and pyroclastic, including many fine volcanic bombs and have erupted a variety of inclusions.

Lava flows near some of the cones are underlain by basaltic ash deposits, over 7m this in places, especially in the region around Panyam.

2. 4 Kassa Volcanic Field

The Kassa volcanic basalt is one of the intraplate basaltic rocks on the Jos Plateau, north central Nigeria. It consists of about eight monogenetic volcanic cones overlying an area of about 66.6Km^2 and an erupted lava volume of about 45.5Km^2 based on geologic mapping and satellite image analysis. The volcanic centers constructed scoria cones and lava flows. The lava flows are mainly boulders of basaltic rocks, scoria and in some cases pumice, micro flow structures are part of these flows. Lar and Tsalha characterized the basaltic rocks in this area as alkaline basalt and grouped the basaltic rocks found in this area as Older and Newer Basalts and therefore, suggested that they erupted during the Quaternary to Tertiary times which is consist with the present work [16].

The petrographic study and microprobe analysis of basaltic rock in thin section revealed the presence of plagioclase laths and magnetite in ground mass, olivine (forsterite), clinopyroxene (diopside) and plagioclase phenocrysts (labradorite) and magnetite and/or ilmenite.

3. Material and Methods

3.1 Introduction

This chapter discusses the procedure used in carrying out the survey and the subsequent analysis of the results obtained. It includes the description of the techniques used in compiling, collating and analyzing the data generated from the study. The procedures involve thin sectioning of the rocks, using to study rocks petrologic microscope under plane and cross-polarised light, chemical analysis using ICPMS, and mathematical computation.

3.3 Methods

The procedures used for data collection are basically from primary source such as rock samples collected along Miango and Kassa volcanoes and secondary source, such as journals, internet, textbooks, etc. The following rock samples of gabbroic composition were collected and their compositions were used to classify them.

3.3.1 Field Mapping and Sample Collection

The study area covers a total area of about 4.5km^2 close to Kassa village from the south along Bukuru – Barkin ladi road to Heipang to the North. The area falls within Naraguta Sheet 168SE, mapped on a scale of 1:10,000. The dominant rock types encountered are: basalts, Older granites, Younger granites and sediments. The Basalts are divided into: Older basalts, Newer basalts and lateralized basalts. The following rock samples of gabbroic composition were collected and their compositions are used to classify them and these are shown in Plate 1, 2, 3, 4, 5, and 6, below.

- Basalt
- Volcanic agglomerate
- Volcanic ash

Plate 1:

Plate 1, below represents a basaltic rock at location 1 in Kassa volcanic field at Jos Plateau state

Plate 1. Showing basalt at Kassa

Plate 2:

Plate 2, below represents a basaltic rock at location 2 in Kassa volcanic field at Jos Plateau state

Plate 2. Showing Volcanic Ash at Kassa

Plate 3:

Plate 3, below represents a basaltic rock at location 3 in Kassa volcanic field at Jos Plateau state

Plate 3. Showing Volcanic Basalt at Kassa

Plate 4:

Plate 4, below represents a basaltic rock at location 4 in Kassa volcanic field at Jos Plateau state

Plate 4. Showing Volcanic Agglomerate at Miango

Plate 5:

Plate 5, below represents a basaltic rock at location 5 in Kassa volcanic field at Jos Plateau state

Plate 5. Showing Volcanic Agglomerate at Kassa

3.4 Methods adopted in this Research

Achuenu and others uses this mathematical equation below to calculate the numerical values of all the minerals in rocks with respect to thermodynamics and this is given as.

$$\sum_{n=0}^{p}\binom{n}{p}\left[\beta\text{-}\alpha\right]_{n+p}(Z_0)_{\bar{\delta}}=\binom{n}{p}\left[\beta_{n-p}\alpha_p\right](Z_0)_{\bar{\delta}}$$

Where Z_0 is the silicate identity and

η = (ionic spacies)

' η ' is the strength of the magma 𝔚 , which is the ratio of the silicate radical z^- to that of cation x^+ under electrolytic condition and 'p' is the recipient cation which depends on ' η '.

$\binom{n}{p}$ Is the coefficient of rock forming minerals and it determines the number of outcomes of each mineral in the melt $M(Z_0)_{\bar{\delta}}$.

3.4.1 Mathematical connection between Bowen's and Goldschmidt concept using Binomial Expansion (Achuenu and others, 2025)

Therefore for:

$$\sum_{n=0}^{p}\binom{n}{p}\left[\beta\text{-}\alpha\right]_{n+p}(Z_0)_{\bar{\delta}}=\binom{n}{p}\left[\beta_{n-p}\alpha_p\right](Z_0)_{\bar{\delta}}$$

$$\sum_{n=r}^{p}\binom{n}{p}\left[\beta\text{-}\alpha\right]_{n+p}(Z_0)_{\bar{o}}=\binom{n}{p}\left[\beta_{n-p}\right]\alpha_0(Z_0)_{\bar{o}}-\binom{n}{p}\left[\beta_{n-p}\right]\alpha_1(Z_0)_{\bar{o}}$$

$$+\binom{n}{p}\left[\beta_{n-p}\right]\propto_2(Z_0)_{\bar{o}}$$

Mathematically, in complex analysis:

$i^2 = -1$

$$\sum_{n=0}^{p}\binom{n}{p}\left[\alpha+\beta\right]_{n+p}(Z_0)_{\bar{\delta}}=\left[\beta_n\right](Z_0)_{\bar{\delta}}+i\left\{\left[\beta_{n-p}\alpha_p\right](Z_0)_{\bar{\delta}}\right\}+\left[\propto_p\right](Z_0)_{\bar{\delta}}$$

' i' is a complex number in silicate Magma.

$({}^{n}c_{p},) = \binom{n}{p}$

$$\binom{n}{p} = \frac{n!}{(n-p)!\,p!} \text{ and } O! = 1$$

δ = o, p, a, m and f

Where, o, p, a. and m are olivine, pyroxene, amphibole, mica and feldspar

3.5 Anhydrous Melt, $\mathfrak{W}$

Magma with no water content at high temperature, silica deficient and low viscosity.

3.5.1 Mathematical Expression for Mafic Olivine Series:

$$\sum_{n=r}^{p}\binom{2}{0}[\alpha+i\beta]_2\,(Z_0)_{\bar{o}} = 1[\beta_2](Z_0)_{\bar{o}} - 2[\beta_1 \propto_1](Z_0)_{\bar{o}} + 1[\propto_2](Z_0)_{\bar{o}}$$

Given that, $\beta = Magnesium$

$\propto = Iron$

Y = Calcium, Chromium, Nickel or Manganese

$(Z_0)_{\bar{o}} = Si\ O_4$

From equation above, we can rewrite it as:

$$\sum_{n=r}^{p}\binom{2}{0}[\alpha+i\beta]_2\ Si\ O_4 = 1\ Mg_2\ SiO_4 + i\{2[\mathrm{MgFe}]\ SiO_4\} + 1\ Fe_2Si\ O_4$$

$$[\mathrm{Mg+iFe}]_2\ Si\ O_4 = Mg_2\ Si\ O_4 + i[Mg\ \mathrm{Fe}]Si\ O_4 + i[\mathrm{MgFe}]SiO_4 + Fe_2\ Si\ O_4$$

$$\sum_{n=r}^{p}\binom{2}{0}[Mg+iFe]_{n+p}\,Si\ O_4 = Forsterite + i[Hyalosiderite] + i[Hortono\ lite] + Fayalite$$

According to Achuenu and others (2025), $Mg_{2-p}Fe_pSiO_4$ is an **'<u>Olivine series</u>'** formula that can be used to calculate all olivine minerals from the melt $\mathfrak{W}$, where p is an integer and ranges from 0 to 2 in olivine crystals. At p equals to zero, 100% Forsterite (Fo) crystallizes with chemical formula of Mg_2SiO_4 and at p equals to 2, Forsterite (fo) disappears and 100% of pure Fayalite (Fa) crystallizes with chemical formula of $Fe_2SiO_{4(s)}$ .Therefore forsterite, *Hyalosiderite* , Hortornolite and fayalite are the primary olivines in the mafic olivine series.

3.5.2 Expected Mathematical Expression for Mafic Pyroxene Series: $[\beta_{2-p}\alpha_p](Z_0)_{\bar{p}}$

$$\sum_{n=r}^{p}\binom{2}{0}[\beta+\alpha]_{2+p}\,Si_2O_6 = 1\,Mg_2Si_2O_6 + i\,[2(MgFe)Si_2O_6] + Fe_2Si_2O_6$$

$$\sum_{n=r}^{p}\binom{n}{p}[\beta+\alpha]_{n+p}\,Si_2O_6 = Mg_2Si_2O_6 + i[Mg\ \mathrm{Fe}]\mathrm{S}i_2\ O_6 + i[MgFe]Si_2O_6 + Fe_2Si_2O_6$$

Pyroxene = Enstatite +Magnesio-hypersthene + Ferro-hypersthene + Ferrosilite

$Mg_{2-p}Fe_pSi_2O_6$ is a pyroxene series, where p range from 0 to 2 in pyroxene. At p equals to zero, 100% Enstatite (En) crystallizes with chemical formula of $Mg_2Si_2O_6$ and at p equals to 2, Enstatite disappears and 100% of pure Ferrosilite crystallizes with chemical formula of $Fe_2Si_2O_6$

Therefore Enstaite, Hypersthene, Eulite and ferrosilite are the primary pyroxenes in the mafic pyroxene series.

3.6 Hydrous Melt

Magma with water content at low temperature, silica saturation and high viscosity

3.6.1 Expected Mathematical Expression for Mafic Amphibole, $[\beta_{7-p}\propto_p](Z_0)_{\bar{a}}2$

$(Z_0)_{\bar{a}} = Si_4O_{11}(OH)^{-7}$

$(Z_0)_{\bar{a}}2 = Si_8O_{22}(OH)_2$

$$\sum_{n=r}^{p}\binom{7}{0}[\beta+\alpha]_7\,(Z_0)_{\bar{a}}2 = 1[\beta_7](Z_0)_{\bar{a}}2 + 7i[\beta_6 \propto](Z_0)_{\bar{a}}2 + 21[\beta_5 \propto_2](Z_0)_{\bar{a}}2 + 30i[\beta_4 \propto_3](Z_0)_{\bar{a}}2$$

$$+30i[\beta_3 \propto_4](Z_0)_{\bar{a}}2 + 21i[\beta_2 \propto_5](Z_0)_{\bar{a}}2 + 7[\beta_1 \propto_6](Z_0)_{\bar{a}}2 + 1i[\propto_6](Z_0)_{\bar{a}}2$$

$$\sum_{n=r}^{p}\binom{7}{0}[Mg+Fe]_7\, Si_8O_{22}(OH)_2 = 1[Mg_7]Si_8O_{22}(OH)_2 + 7i[Mg_6Fe_1]Si_8O_{22}(OH)_2$$

$$+21[Mg_5Fe_2]Si_8O_{22}(OH)_2 + 30i[Mg_4Fe_3]Si_8O_{22}(OH)_2 + 30[Mg_3Fe_4]Si_8O_{22}(OH)_2$$

$$+21i[Mg_2Fe_5]Si_8O_{22}(OH)_2 + 7[MgFe_6]Si_8O_{22}(OH)_2 + 1i[Fe_6]Si_8O_{22}(OH)_2$$

Then:

$[\beta_{7-p} \propto_p](Z_0)_{\bar{a}}2$ = [($Mg_{7-p}Fe_p$)($Si_8O_{22}(OH)_2$)]

According to Achuenu and others, ***[($Mg_{7-p}Fe_p$)($Si_8O_{22}(OH)_2$)*]** is a chemical formula for an Amphibole series, when p ranges from 0 to 7. At p equals to zero, 100% of Kupfferite (Ku) with chemical formula of $Mg_7Si_8O_{22}(OH)_2$ crystallizes. At p equals 7, Kupfferite disappears, and 100% pure Grunerite (Gr) crystallizes with chemical formula of $Fe_7Si_8O_{22}(OH)_2$

3.6.2 Mathematical Expression for Mafic Mica Series: $[\beta_{6-p} \propto_p](Z_0)_{\bar{m}}2$

The crystal of amphibole interacts with the magma, so that the **$Si_4O_{11}(OH)$** of amphibole links to cation is being hydrolyzed in the presence of excess water in the magma as shown in equation below

$Si_4O_{11}(OH)(aq) + 0H_{(aq)} \longrightarrow Si_4O_{10}(OH)_2(aq)$

$(Z_0)_{\bar{a}}2 = Si_4O_{20}(OH)_4$

$$\sum_{n=r}^{p}\binom{6}{0}[Mg_6]Si_4O_{20}(OH)_4 + 6i[Mg_5Fe_1]Si_4O_{20}(OH)_4 + 15[Mg_4Fe_2]Si_4O_{20}(OH)_4$$

$$+20i[Mg_3Fe_3]Si_4O_{20}(OH)_4 + 15[Mg_2Fe_4]Si_4O_{20}(OH)_4 + 6i[Mg_1Fe_5]Si_4O_{20}(OH)_4 + 1[Fe_6]Si_4O_{20}(OH)_4$$

Mafic Mica = Phlogopite + i[Magnesio-biotite]+ Biotite +i[Ferro-biotite]+ Lepidomelane

$[\beta_{6-p}\alpha_p](Z_0)_{\bar{m}}2$ = [$Mg_{6-p}Fe_p$][$Si_8O_{20}(OH)_4$]

According to Achuenu and others (2025), ***[$Mg_{6-p}Fe_p$][$Si_8O_{20}(OH)_4$]*** is a biotite series, as p ranges from 0 to 6. At ‘p’ equals to zero, 100% of phlogopite (Ph) crystallizes, and at ‘p’ equals to 7, Phlogopite (Ph) disappears and 100% pure Lepidomelane (Lp) crystallizes with a chemical formula of $K_2Fe_6Al_2Si_6O_{20}(OH)_4$.

3.6.3 Expected Mathematical Expression for Plagioclase Series

$(\Upsilon_{m-p}X_p)(Q_{x-y}N_y)W_i$

$(\Upsilon+X)_{x+y}\ W_i = (\Upsilon_{m-p}X_p)(Q_{x-y}N_y)W_i$

$[X_{m-p}\Upsilon_p]Zi = [X_{1-p}\Upsilon_p](Z_0)_{\bar{f}}2$

$= [X_{m-p}\Upsilon_p](Z_0)_{\bar{f}}2$

$(Z_0)_{\bar{f}}2 = S_iO_4$

$(Z_0)_{\bar{f}}2 = S_{i\,4}O_8$

Υ−Position $=\Upsilon+X$

$[X_{m-p}\Upsilon_p](Z_0)_{\bar{f}}2 = [X_{1-p}\Upsilon_p][Q_{4-y}N_y]W_i$

For p = 1 and y =1

$[X_{1-p}\gamma_p][Q_{4-y}\mathcal{N}_y]\mathcal{W}_i = [X_{1-1}\gamma_1][Q_{4-1}\mathcal{N}_1]\mathcal{W}_i$

$[X_{1-p}\Upsilon_p][Q_{4-y}N_y]W_i = [\Upsilon_1][Q_3N_1]W_i$

$\gamma_m[Q+\mathcal{N}]_{x+y} + [x]_p(Q+\mathcal{N})_{x+y} = [X_{1-p}\gamma_p][Q_{4-y}\mathcal{N}_y]\mathcal{W}_i$

$\gamma_m[Q+\mathcal{N}]_{x+y}+[x]_p(Q+\mathcal{N})_{x+y}$ is called "***<u>PLAGIOCLASE SERIES</u>***"

$\gamma_m[Q+\mathcal{N}]_{x+y}+[x]_p(Q+\mathcal{N})_{x+y} = CaAl_2Si_2O_8 + NaAlSi_3O_8$

Equation (87), is used to solve the problem involving couple substitution in felsic rock.

3.7 Application of Metrical Matrices to Rock Forming Minerals

3.7.1 Metrical Matrix for Mafic Olivine and Feldspars

Then set equations (105)*and* (110)*in matrices form*.

$[\Upsilon_1(Q_2\,N_2)]0_8+X_1(Q_3\,N)0_8=[(1,\ 0],[2,\ 0)]+[(0,\ 1],[3,\ 1)]$

$[\beta_2](Z_0)_{\bar{o}}+[\alpha_2](Z_0)_{\bar{o}}=[2,0]+[0,2]$

$$\begin{bmatrix} Anorthite \\ Forsterite \end{bmatrix} + \begin{bmatrix} Albite \\ Fayalite \end{bmatrix} = \begin{bmatrix} Anorthoclase \\ Olivine \end{bmatrix}$$

3.7.2 Metrical Matrix for Mafic Pyroxene and Feldspar

$$\begin{bmatrix} Anorthite \\ Enstatite \end{bmatrix} + \begin{bmatrix} Albite \\ Ferrosilite \end{bmatrix} = \begin{bmatrix} Anorthoclase \\ Pyroxene \end{bmatrix}$$

3.7.3 Metrical Matrix for Mafic Amphibole and Feldspar

… (127)

… (128),

$$\begin{bmatrix} \mathrm{Ca}_1[Al_2\,Si_2]0_8 \\ \\ [Mg_7]Si_8O_{22}(OH)_2 \end{bmatrix} + \begin{bmatrix} \mathrm{Na}_1[AlSi_3]0_8 \\ \\ [Fe_2]Si_8O_{22}(OH)_2 \end{bmatrix} = \begin{bmatrix} [(\mathrm{Ca}_1\mathrm{Na}_1)(Q_5\,N_3)]0_{16} \\ \\ [MgFe]_7Si_{16}O_{44}(OH)_4 \end{bmatrix}$$

$$\begin{bmatrix} Anorthite \\ Kupfferite \end{bmatrix} + \begin{bmatrix} Albite \\ Grunerite \end{bmatrix} = \begin{bmatrix} Anorthoclase \\ Anthophyllite \end{bmatrix}$$

3.7.4 Metrical Matrix for black Mica and Feldspar

… $(Z_0)_{\bar{m}}$ (134)

… (135),

$$\begin{bmatrix} Anorthite \\ Phlogopite \end{bmatrix} + \begin{bmatrix} Albite \\ Lepidomelane \end{bmatrix} = \begin{bmatrix} Anorthoclase \\ Biotite \end{bmatrix}$$

4. Mathematical Concept of Rock Forming Minerals

4.1 Introduction

Based on the chemical analyses and the examination under thin section, Kassa basalts are classified into alkaline, olivine basalt magma type and tholeiite magma type

1. Olivine Basalt Magma Type:
The essential minerals are olivine, augite, basic plagioclase, and iron ore. The pyroxene is a Diopside or basaltic augite often a titaniferous variety.
2. Tholeiite Basalt Magma Type:
The essential minerals are pyroxene, basic plagioclase and iron ore. Olivine is either completely absent or present in very subordinate amount. The pyroxene belongs typically to the enstatite – augite (pigeonite) series of lime - poor pyroxene.

Yoder and Tilley comment that in alkali basalts the total alkalis usually exceed 3%. In some siliceous tholeiites the alkalis exceed 3%, whereas some silica-poor alkali basalts contain less than 3% total alkalis [17]. Therefore, alkali basalt contains normative olivine and nepheline that is 3%<Ne<5%. Ne > 5% is called Basanite. Tholeiite basalt contains less than 5% modal olivine, tholeiite olivine basalt contains greater than 5% modal olivine and alkali basalt contains less than 5% modal olivine. The tholeiite basalt is characterized by the existence of reaction relation between the Mg.

Olivine and Ca-poor pyroxene, namely orthopyroxene and pegionite. Therefore, Mg olivine is usually absent from the ground mass of volcanic rock, where present, it is surrounded by the reaction rims of pegionite provided that the groundmass is reasonably crystalline. Alkali olivine basalt is characterized by the absence of reaction relation between olivine and pyroxene, olivine is invariably present in the groundmass.

4.2 Results and Interpretation Using Mathematical Methods

The rock samples that were collected from Kassa basalt were chemically analyzed using inductively coupled Plasma - Mass Spectrometer (ICP-MS) method in Canadian laboratory with their known temperatures measured in degrees and the results are presented in table 2, 3 and 4 below.

Parameters such as total relative bonding, ionic charge, and ionic radius of elements as shown Table 6 The nucleation and growth of crystals from basaltic melt depend on these parameters with respect to temperature of crystallization under isobaric condition. The principal minerals in basalt are the basic plagioclase, basic olivine, and basic pyroxene, that is,"CaMg rich minerals

Table 2. Partition Coefficientof of Various Trace elements

Trace Element	Atomic radius	Ioniic Charge	Concentration in Solid(S)	Concentration in Liquid(L)	Partition Coefficient(D)
Nickel	0,69	+2	10	**1**	**4 – 10**
Titanium	**0.68**	**+4**			
Cromium	0.63	+3	1	5	0.2
Iron	0.74	+2			
Robidium	1.47	+1			
Strotium	1.12	+2	1	100	0.001
Zircon	0.79	+4			
Fluorine	1.33	-1			
Chlorine	1.81	-1			

Table 3. Major Oxides Compositions of KASSA and MIANGO Basalts

Mineral			Percentage composition of normative minerals of selected Basalts					Percentage Composition of normative minerals as it is observed from Thin Section by counting under Microscope and chemical analysis.									
			Olivine basalt Magma Type	Tholeiitic Magma Type	Tristan Olivine basalt, P.E.Baker et al, (1964).	Hualalai Alkali basal, Yolde and Tilley (1962) .	Kilauea Tholeiite, Yoder and Tilley, (1962)	KASSA					MIANGO				
S/N	**Geologic Name**	**Genetic Type**	**1**	**2**	**3**	**4**	**5**	**KIA1**	**KIA2**	**KIA3**	**KIA4**	**KIA5**	**MIA1**	**MIA2**	MIA3	MIA4	MIA5
1	Quartz			0.0	0.0	0.0	0.3	0.0	0.0	0.0	0.0	0.0	0.0	0.0	0.0	0.0	0.0
	Olivine			5	10.6	18.5	0.0	8.0	0.0	0.0	14.0	35	35	20.0	17	0.0	0.0
2	Pyroxene	Augite			29.1	20.9	22.0	17.0	1.0	4.0	11.0	10.0	10.0	0.0	0.0	0.0	0.0
3		Clino-pyroxene		51	0.0	0.0	22.4	0.0	0.0	20	0.0	0.0	0.0	10.0	10	45.0	45.0
4	Plagioclase Feldspar	Labradorite		30	0.0	0.0	0.0	21.0	0.0	25	22.5	12.5	20	0.0	0	15’0	12.5
5		Bytownite			0.0	0.0	0.0	26	1.0	26	27.5	17.5	25	0.0	5	20.0	17.5
		Anorthite			20.4	23.6	26.1	0.0	0,0	0.0	0.0	0.0	0.0	0.0	0.0	0.0	0.0
	Alkali Feldspar	Albite			3.2	20,0	21.0	0.0	0.0	0.0	0.0	0.0	0.0	0.0	0.0	0.0	0.0
		Orthoclase			12.2	5.3	2.2	0.0	0.0	0.0	0.0	0.0	0.0	0.0	0.0	0.0	0.0
6	Opaque	Magnetite		9	4.1	4.5	1.9	7.0		25.0	25.0	25.0	10.0	0.0	0.0	20.0	20
7		Ilmenite			7.9	4.3	3.0	0.0	0.0	0.0	0.0	0.0	0.0	0.0	0.0	0.0	0.0
8	Feldsparthoid	Nepheline			11.1	2.2	0.0	0.0	0.0	0.0	0.0	0.0	0.0	0.0	0.0	0.0	0.0
	Rest			5	0.0	0..1	0.1	+21	+97	0.0	0.0	0.0	0.0	+70.0	+68	0.0	0.0
9	Apatite				1.4	0.7	0.3	0.0	0,0	0.0	0.0	0.0	0.0	0.0	0.0	0.0	0.0

Table 4. Chemical Analysis of kassa Basalt using ICPMS

.	Chemical Expression	Percentage composition of normative minerals of selected Basalts					Percentage Composition of normative minerals as it is observed from Thin Section by counting under Microscope and chemical analysis.					
		Olivine basalt Magma Type	Tholeiitic Magma Type	Tristan Olivine basalt, P.E.Baker et al, (1964).	Hualalai Alkali basal, Yolde and Tilley (1962) .	Kilauea Tholeiite, Yoder and Tilley, (1962)	KASSA					Conversi on Factors
	Sample	1	2	3	4	5	KIA1	KIA 2	KIA3	KIA4	KI A5	
15	SiO2	45.0	50.24	42.78	46..53	51.18	52.00		50.57	50.78	49.0 5	0.467439
16	TiO2	0.0	2.65	4.14	2.28	2.10	2.26		2.88	2.38	2.30	0.599508
17	Al2O3	15.0	13.32	14.27	14.31	14.07	14.23		17.30	15.23	14.6 4	0.529251
18	Fe2O3/FeO	13.0	9.85	5.89	3.16	1.35						
19	FeO/Fe2O3		1.41	8.55	9.81	9.78	10.25		10.89	11.29	11.0 9	0.699433
20	MnO		0.17	0.17	. 0.18	0.17						
21	MgO	8.0	8.39	6.76	9.54	7.78	7.10		3.30	8.03	8.39	0.603036
22	CaO	9.0	10.84	12.01	10.32	10.83	8.50		8.30	8.73	9.60	0.714701
23	Na2O	2.5	2.32	2.79	2.85	2.39	3.34		4.32	2.90	3.52	0.741857
24	K2O	0.5	0.54	2.06	0.84	0.44	1.13		1.52	1.52	1.41	0.830147
25	H2O+				0.08	0.10						
	P2O5		0.27	0.58	0.28	0.15	0.33		0.84	0.66	0.58	0.436421
To tal												

Table 5. Typical Partition Coefficient of Trace Elements between Crystals and Liquid in KASSA Basalts

	Tra ce Ele me ntl		Trace elements in Basaltic liquid: from J.G., Arth, 1976, Jour.Res.U.S. Geol. Surv. ,4: 41-47.							Trace elements in Basalt of KASSA from the researcher.				
		Oliv ine	**Pyrox ene**	Pyrox ene	Amphibol e	Mica	Plagioc lase	Spine l	Garnet	Converted Data in KASSA x100				
S/ N		*1*	2	3	*4*	*5*	6	*7*	*8*	*KIA1*	*KIA 2*	*KIA 3*	*KIA4*	
1	Ni	4-10	8.3	2.5	6.0	7.6	0.05	5.0	0.5	1.54		0.17	1.68	
2	Cr	0.2	2.0	11.5	5.2	7.0	0.06	10.0	2.0	2.26		0.07	1.72	2.1 5
3	Co	3.9	2.4	1.0	6.5	1.1	0.05	2.0	3.2	0.46		0.35	0.49	0.5 0
4	Sc	0.2	1.2	2.7	3.5	3.0	0.03	2.0	3.4					
5	Sr	0.01	0.03	0.11	0.6	0.1	2.1	<0.1	<0.1	4.45		9.59	6.63	7.8 1
6	Ba	0.02	0.05	0.02	0.4	<0.1	0.38	<0.1	<0.1	4.23		8.77	8.89	5.1 1
7	Rb	0.02	0.006	0.03	0.4	2.0	0.09	<0.1	<0.1					
	Mn									1.17		1.35	1.43	1.3 5
	Zr									1.56		2.71	1.92	1.9 7
	V									1.69		1.93	1.69	1.6 7
	Zn									1.07		1.33	1.17	1.3 1

Explanation of Column Headings

KIA1: Alkaline Olivine basalt, Kassa, Barkinladi, plateau state.

KIA2: Volcanic Tuff, Kassa, Barkinladi, Plateau state.

KIA3: Tholeiite basalt, Kassa, Barkinladi, Plateau state.

KIA4: Olivine basalt, Kassa, Barkinladi, Plateau state.

KIA5: Alkaline Olivine basalt, Kassa, Barkinladi, Plateau state.

Table 6. Showing the Relative bonding, Ionic radius, Ionic charge, Ionization and Electronegativity of elements

Element	Electronegetivity	Ionization Energy	Ionic radius	**Ionic Charge**	**Total Relative Bonding**
Sodium	0.90	5.133	0.97	**+1**	**100**
Potassium	***0.80***	***4.339***	***1.33***	***+1***	***90***
Magnesium	1.20	14.970	0.66	+2	202
Calcium	1.0	11.820	0.99	+2	200
Aluminium	1.50	28.31	0.51	+3	300
Cromium	1.50/1.40	15.700	0.63	+3	321
Manganese	1.60	32.100	0.80	+2	174
Iron	1.65	16.240	0.644	+2	174
Iron	1.80		0.74	+3	
Nickel	1.8/1.7	18.130	0.69	+2	1.97
Silicon	1.80	44.950	0.42	+4	380
Cobalt	1.80/1.70	17.300		+2	183
Chlorine	3.0		1.81	-1	
Fluorine	4.0		1.33	-1	
Oxygen	3.50			-2	384

4.3 Application of Mathematical Principles to Geology of Kassa Volcanic Field of Jos Plateau State.

1. Petrographic study of Kassa, Jos Plateau state

The rock samples that were collected from KASSA Volcanic Field were prepared into thin Section and studied under petrologic microscope. Observations as the rock characteristics were made under plane and cross polarized light. Details of the observations made are given below.

Rock KIA1:

Texture: porphyritic texture with presence of vesicles

Colour: dark to grey

Mineral composition: plagioclase, olivine and pyroxene are the main minerals with no quartz. Iron ore is also present.

(b) Thin section.

Slide KIA1:

Texture: Porphyritic, Vesicular, and the groundmass is intergranular (the spaces between the plagioclase laths are occupied by one or more grains of pyroxene and olivine). Vesicles are irregular with some showing flow defomation as shown in Plate 6 and 7.

20% porphyritic consisting:

Aug (5%), Ol (8%), Pl (7%).

The olivines and pyroxenes are rounded by rims (pigionite?)

The plagioclase phenocrysts show zonation.

77% groundmass (neglecting vesicles) consisting

40% Pl which are euhedral to subhedral shaped

12% Aug which are subhedral to anhedral

7% Op, which exhibits anhedral enlogate shape (ilmenite?)

Crystallinity: Hypocrystalline.

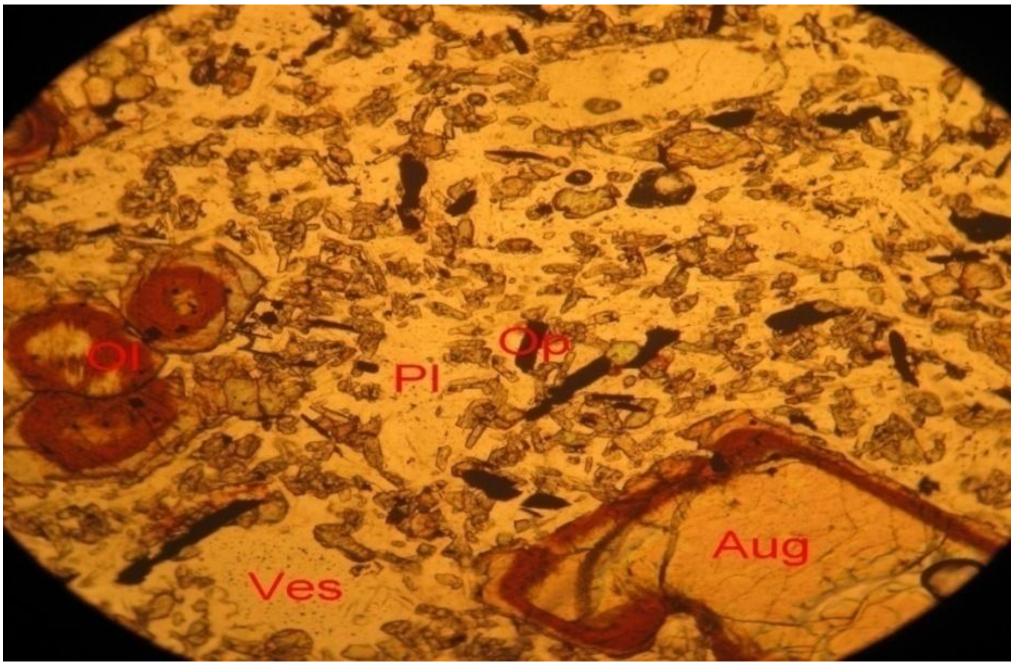

Slide KIA1a. Photomicrograph of KIA 1, PPL showing the olivines and pyroxenes are rounded by rims (pigeonite?)

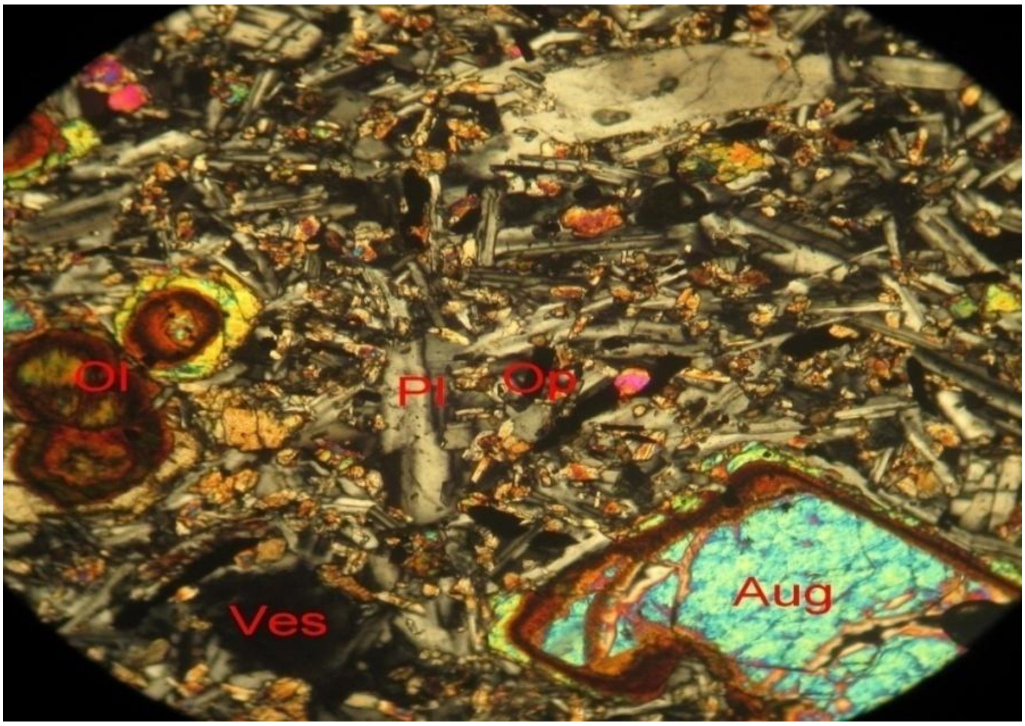

Slide KIA1b. Photomicrograph of KIA 1, XPL showing the olivine and pyroxenes are rounded by rims (pigeonite?)

Rock KIA2:

Texture: Volcanic ash

Colour: white to grey

Slide KIA2.

Texture: Very few phenocrysts of clinopyroxenes (augite) present at quite some distance from one another as shown in Plate 8 and 9. The crystals (skeletal) have fracture filled with brown opaque material resulting from alteration.

> 1% phenocrysts of augite

> 98% groundmass (neglecting vesicles) consisting:

> 97% dark brown to brown volcanic glass populated with tiny grains of opaques minerals, few quartz and pyroxenes

< 1% Pl. The plagioclase laths are fine-grained subhedral shaped and are present in a particular portion of the rock.

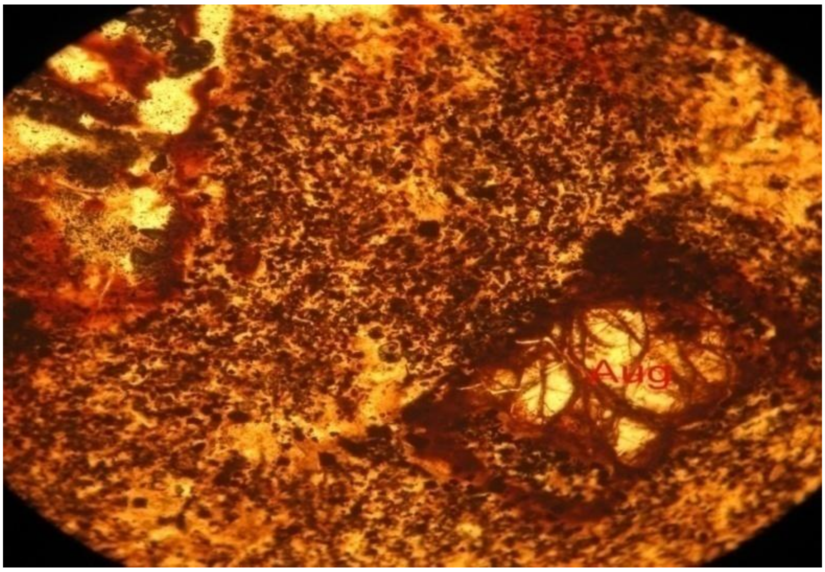

Slide KIA2a. Photomicrograph of KIA 2, PPL very few phenocrysts of clinopyroxenes (augite)

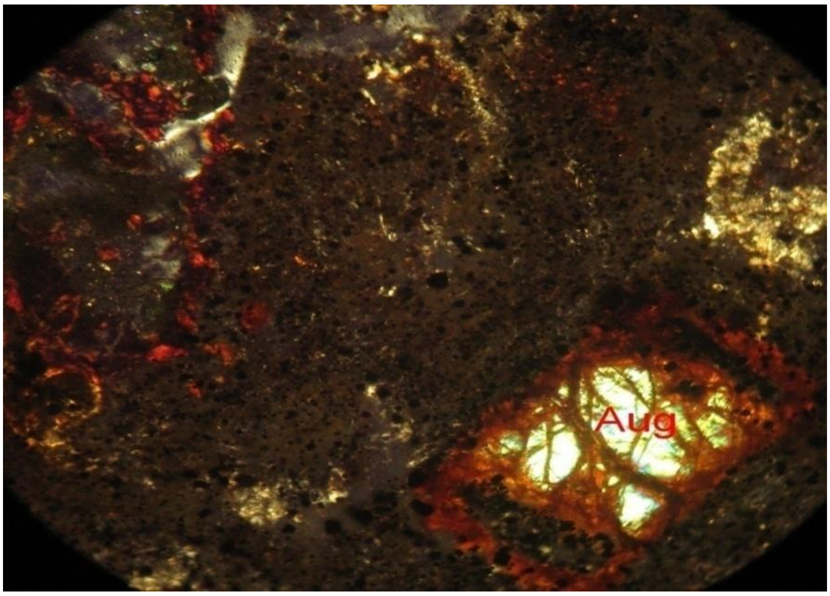

Slide KIA12. Photomicrograph of KIA 2, XPL, very few phenocrysts of clinopyroxenes (augite)

Rock KIA3

Texture: fine grained rock with presence of vesicles

Colour: dark grained rock.

Mineral composition: Plagioclase, olivine and pyroxene are the main minerals with no quartz. Iron ore is also present.

Slide KIA3

Texture: Microphenocrysts of clinopyroxenes and plagioclases some of the augite grains have been and are being replaced (brown – yellow) by secondary minerals (chlorite?). there is presence of rounded vesicles as shown in Plate 10 and 11.

< 5% microphenocrysts, consisting:

< 4% aug and >1% Pl

> 95% groundmass (veglecting vesicles), consisting:

> 50% Pl laths that show moderate alignment in a common plane and euhedral to subhedral shaped

< 20% Cpx –which are subhedral to euhedral shaped

< 25% Op which are tiny and rounded (magnetite?)

Crystallinity: Hypocrystalline.

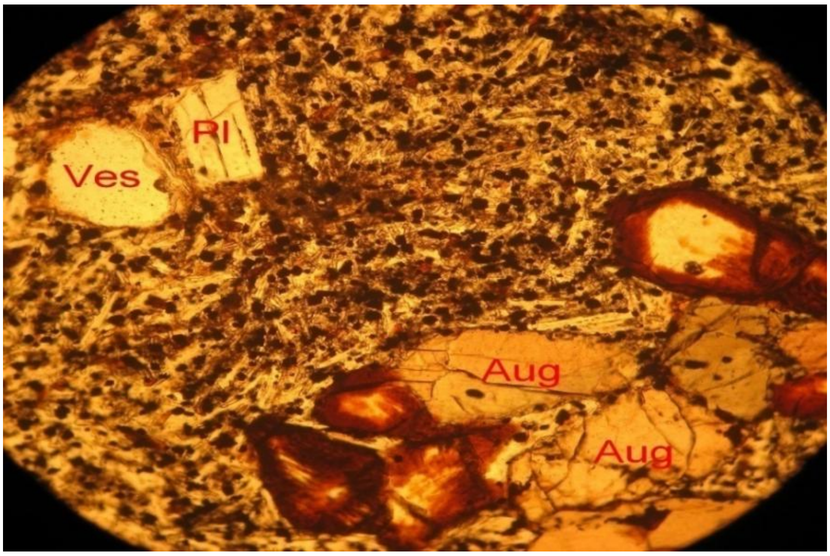

Slide KIA13a. Photomicrograph of KIA 3, PPL microphenocrysts of clinopyroxenes and plagioclases

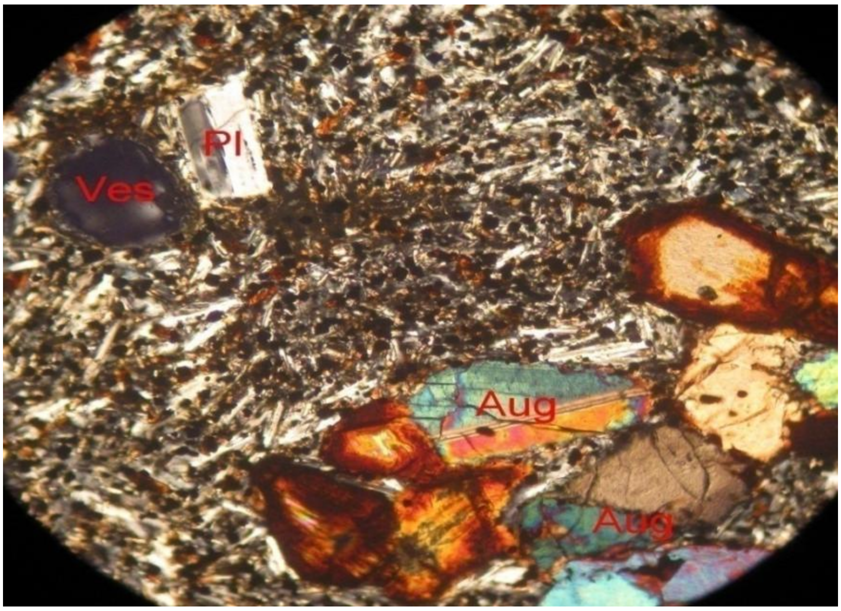

Slide KIA1b. Photomicrograph of KIA 3, XPL microphenocrysts of clinopyroxenes and plagioclases

Rock KIA4:

Texture: very fine grained rock, euhedral to subhedral in shape

Colour: dark in colour and vesicular

Mineral composition: Plagioclase, olivine and pyroxene are the main minerals with no quartz. Iron ore is also present.

Slide KIA4

Texture: Phenocrysts of Augite and olivine, tiny vesicles, and groundmass.

$<$ 20% Phenocrysts, consisting:

$<$ 14% Ol which are euhedral to subhedral shaped

$>$ 6% Aug which are euhedra to subhedral shaped

$>$ 80% Groundmass consisting:

$<$ 50% Very fine-grained needled-like plagioclase laths showing slight alignment in a common plane

$<$ 5% Aug + Ol

$<$ 25% tiny rounded opaque (magnetite?)

Crystallinity: Hypocrysalline.

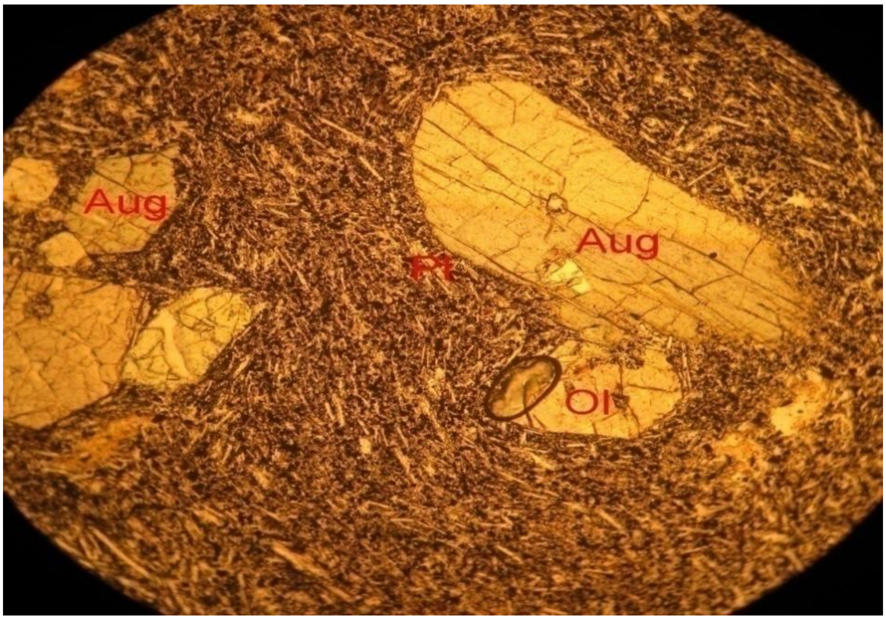

Slide KIA4a. Photomicrograph of KIA 4, PPL phenocrysts of augite and olivine

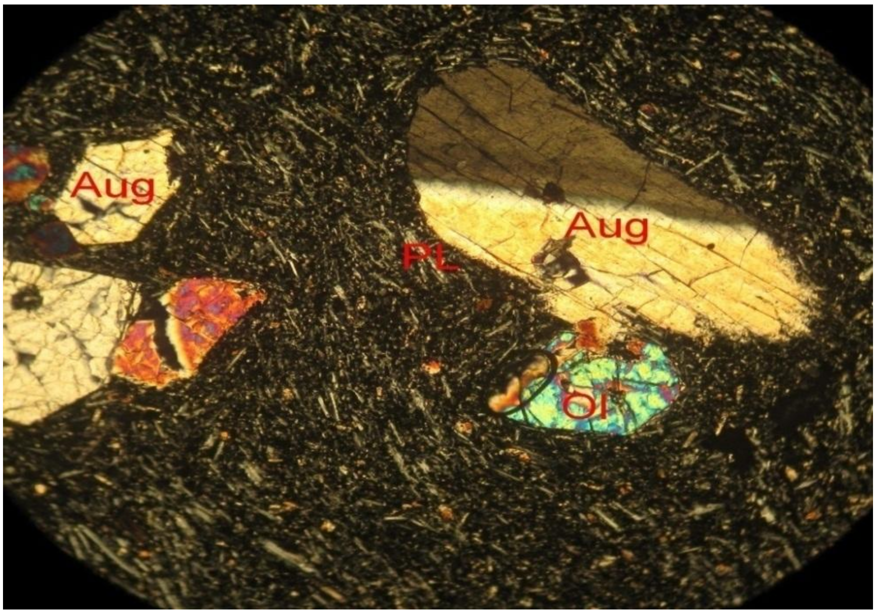

Slide KIA14b. Photomicrograph of KIA 4, XPL phenocrysts of augite and olivine

Rock KIA5:

Texture: fine grained rock with presence of vesicles

Colour: dark to grey

Mineral composition: plagioclase, olivine and pyroxene are the main minerals with no quartz. Iron ore is also present.

Slide KIA5

Texture: Phenocrystals of olivine and Augite with euhedral to subhedral shapes as shown in Plate 14 and 15.

>30% Phenocrysts consisting:

> 20% Ol and < 10% Aug

< 70% Groundmass (Neglecting Vesicles) consisting:

> 30% Pl which are needle-like laths showing slight alignment in a common plane

> 15% Ol + Aug

< 25% tiny opaque (magnetite?)

Crystallinity: Hypocrystalline.

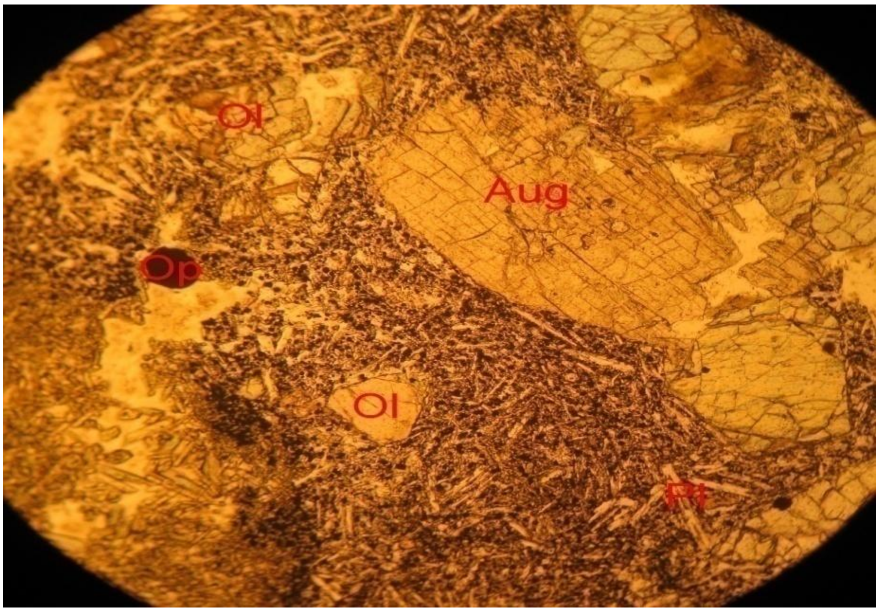

Slide KIA5a. Photomicrograph of KIA 5, PPL phenocrystals of olivine and augite

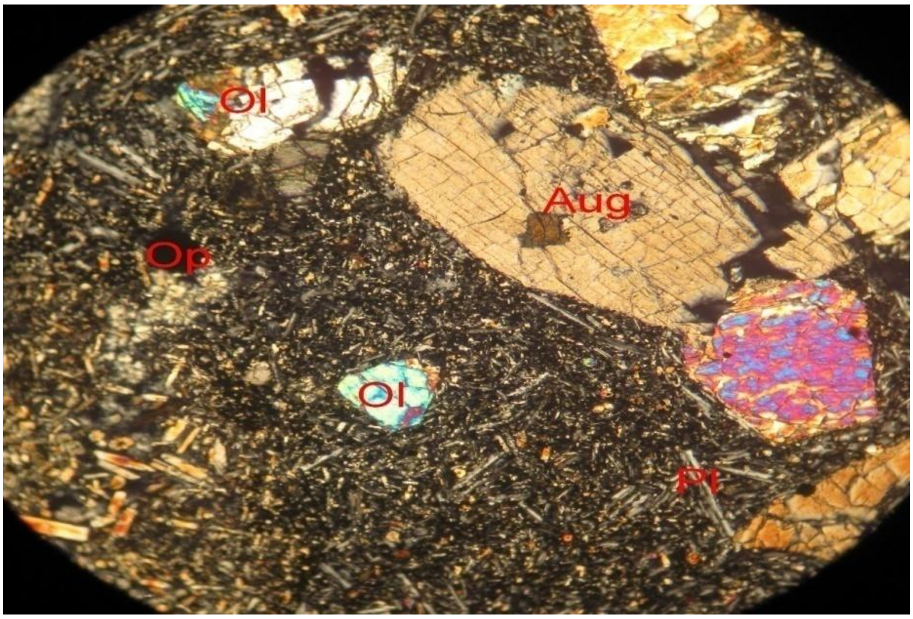

Slide KIA5b. Photomicrograph of KIA 5, XPL phenocrysts of olivine and augite

4.4 Mathematical Analysis of Mafic, Felsic and Ferrous/Ferric Minerals of KIA1 in Kassa Volcanic Field

In **Kassa Volcanic Field,** the expected rock type of **KIA1** is "**Alkali Olivine basalt**" becauses the modal olivine as observed under microscope both plane and crossed polarized light is greater than **5%** as seen in Table 3 above and the total alkali content analysed using ICP-MS exceeds **3%** as seen in Table 4 above and as commented by Yoder and Tilley (1962, p. 355). The compositions of alkali olivine basalt of **KIA1** include:

1.Plagioclase, **Andesine. (47%)**
2.Olivine, **Hyalosiderite (8%)**
3.Pyroxene, **Augite.(17)**
4.Iron ore, **Ulvospinel,** which is titanite granular magnetite (**7%**).
Alkali olivine basalt is likely to be produced by the partial melting of the upper mantle material at the depth of about 80km and an average temperature of 1250^0C.

Olivine crystallizes first, as the first fraction. It forms with its silicon arranged in isolated tetrahedrons of SiO_4 with a general chemical formula of **$(MgFe)_2SiO_4$** ranging from **Mg_2SiO_4** (forsterite) to **Fe_2SiO_4** (fayalite) as shown in Appendix A in A1, olivine has proportions of one-part silicon to two parts iron or magnesium [1:2 ratios], which means it depletes the magma of iron and magnesium and leaves the remaining liquid with proportionately more silicon. Olivine has a general molecular formula of $(\beta_{2-p}\alpha_p)Z_0$ and when the sample of **KIA1** collected from Kassa volcanic basalt observed under thin section, its modal percentage composition is (**8%**) as shown in Table 4 above.

Pyroxene has a general molecular formula of **(** $\beta_{2\ \mathbf{-p}}\ \alpha_{p}$ **)** $\mathbf{Z_0}$ and when the sample of **KIA1** collected from Kassa volcanic basalt observed under thin section, its modal percentage composition is (**17%**) as shown in Table 4 above.

4.4.1 Empirical formula and classifications for Mafic Oxides of Olivine of KIA1 in Kassa Volcanic Field using Zero Polynomial of ($\beta_{2\ -p}\ \alpha_p$) $(Z_0)_o^-$

Table 4 above, represents the chemical compositions of Oxides of Olivine of KIA1 as analyzed using ICP-MS and can be mathematically analyzed using empirical formula below:

A: Empirical Formula for the Mafic Oxides of Olivine of KIA1

Therefore, the volume percent of Mafic Oxides in KIA1 are:

MgO = **7.10%** in KIA1

FeO = **10.25%** in KIA1

SiO_2 = **52.0%** in KIA1

7.1% + 10.25% + 52.0% = 69.35%

Therefore, the chemical compositions of mafic oxides of Olivine can be expressed using empirical formula as shown Table 7 below.

Table 7. Empirical Formula for the Mafic Oxides of Olivine of KIA1

Oxides of the mineral	MgO	FeO	SiO_2
% composition of the Oxides	**10.24**	14.78	**74.98**
Molar mass of the Oxides	**40**	**68**	**60**
$\frac{\%composition}{Molar\ mass}$	$\frac{10.24}{40}$	$\frac{14.78}{68}$	$\frac{74.98}{60}$
Ratio of the Oxides	**0.256**	**0.217**	**1.25**
Divide by the smallest number	$\frac{0.256}{0.217}$	$\frac{0.217}{0.217}$	$\frac{1.25}{0.217}$
	1.2	**1**	**5.8**
	6	**5**	**29**
	$\mathbf{(MgO)_6}$	$\mathbf{(FeO)_5}$	$\mathbf{(SiO_2)_{29}}$
	$\mathbf{Mg_6O_6}$	$\mathbf{Fe_5O_5}$	$\mathbf{Si_{29}O_{58}}$
Empirical formula of the Oxides	$\mathbf{(Mg_6Fe_5)O_{11}}$		$\mathbf{Si_{29}O_{58}}$
Chemical formula of the mineral	$\mathbf{(Mg_6Fe_5)Si_{29}O_{69}}$		
Mineral 1	**Olivine**		
Mineral 1 + SiO_2	$\mathbf{(Mg_6Fe_5)Si_{30}O_{71}}$		
Mineral 2	**Pyroxene**		

a.$(Mg_6Fe_5)Si_{29}O_{69}$ can be converted to true value of Olivine Mineral using Zero polynomial of $Mg_{2-p}Fe_pSiO_4$
Therefore:

$Mg_{2-p}Fe_pSiO_4$ = $\mathbf{(Mg_6Fe_5)Si_{29}O_{69}}$

$Mg_{2-p}Fe_pSiO_4$ = $\mathbf{(Mg_{11}Fe_9)(SiO_4)_{10}}$

$\mathbf{(Mg_{11}Fe_9)(SiO_4)_{10}}$ **= 8%(Hyalosiderite)**

100% (Hyalosiderite) = 55%(Forsterite) + **45%** (**Fayalite**) as shown in Table 7a, above.

Therefore, For 8%(Hyalosiderite)

8% (Hyalosiderite) = **4.4%(Forsterite)** + **3.6%** (**Fayalite**) **of KIA1** in **Kassa Volcanic Field**

b.$(Mg_6Fe_5)Si_{29}O_{69}$ can be converted to real value of Olivine Mineral using Binomial Expansion of $Mg_{2-p}Fe_pSiO_4$

$$\sum_{p=r}^{n}\binom{2}{0}[\alpha+i\beta]_2\ Si\ O_4 = 1Mg_2\ Si\ O_4 + i\{2[MgFe]\ Si\ O_4\} + 1Fe_2SiO_4$$

$\mathbf{(Mg_6Fe_5)Si_{29}O_{69}}$ can occur in two different ways provided that, the theory of zero polynomial is satisfied during crystallization of magma, either:

$\mathbf{Mg_{10}Fe_{10}Si_{10}O_{40} = Mg_{11}Fe_9Si_{10}O_{40}}$ **Or** $\mathbf{Mg_{10}Fe_{10}Si_{10}O_{40} = Mg_9Fe_{11}Si_{10}O_{40}}$

$[Mg+iFe]_{20}Si_{10}O_{40} = Mg_{20}Si_{10}O_{40} + i[Mg_{11}Fe_9]Si_{10}O_{40} + i[Mg_9Fe_{11}]Si_{10}O_{40} + Fe_{20}Si_{10}O_{40}$

$\mathbf{Mg_{11}Fe_9Si_{10}O_{40}}$ **= Hyalosiderite**

$Mg_9Fe_{11}Si_{10}O_{40}$ = Hortonolite

B: Classification of Mafic Olivine of KIA1 in Kassa Volcanic Field

➢**Olivine class** = 1[basic '**Olivine**'] + [intermediate '**Olivine**'] + i[acidic **Olivine**].
➢**Olivine Minerals** = [basic '**Forsterite]** '+ i[intermediate '**Hyalosiderite**'] + i[intermediate '***Hortonolite*** '] acidic '***Fayalite***'
['**Hyalosiderite** '] = [intermediate '**Olivine**']
['**KIA1** '] = [intermediate '**Hyalosiderite**']
['**KIA1** '] = [intermediate '**Olivine** ']
$Mg_{2-p}Fe_pSiO_4$ is an **'Olivine series'** formula that can be used to calculate all olivine minerals from the melt $\mathfrak{W}$, where p is an integer and ranges from 2 to 0 in olivine crystal. At certain value of p, Hyalosiderite crystallizes with chemical formula of **$(Mg_{11}Fe_9)Si_{10}O_{40}$**. Therefore **8%** of **Hyalosiderite** is the primary olivine in the mafic olivine series of **KIA1** in **KASSA** basalt.

4.4.2 Empirical formula and classifications for Mafic Oxides of Pyroxene of KIA1 in Kassa Volcanic Field using Zero Polynomial of $(\beta_{2-p}\alpha_p)(Z_0)^-_p$

Table 7 above, represents the chemical compositions of Oxides of Pyroxene of KIA1 as analyzed using ICP-MS and can be mathematically analyzed using empirical formula below:

A: Empirical Formula for the Mafic Oxides of Pyroxene of KIA1

a. $(Mg_6Fe_5)Si_{30}O_{71}$ can be converted to true value of Pyroxene Mineral using Zero polynomial of $Mg_{2-p}Fe_pSi_2O_6$
Therefore:

$Mg_{2-p}Fe_pSi_2O_6 = (Mg_6Fe_5)Si_{30}O_{71}$

$(Mg_{11}Fe_9)Si_{20}O_{60} = (Mg_6Fe_5)Si_{30}O_{71}$

$(Mg_6Fe_5)Si_{30}O_{71} = (Mg_{11}Fe_9)Si_{20}O_{60}$

$(Mg_6Fe_5)Si_{30}O_{71} \sim (Mg_6Fe_5)(Si_3O_7)_{11}$

$(Mg_6Fe_5)(Si_3O_7)_{11} = (Mg_{11}Fe_9)(SiO_3)_{20}$

$Mg_{2-p}Fe_pSiO_4 = (Mg_{11}Fe_9)(SiO_3)_{20}$

$(Mg_{11}Fe_9)(SiO_3)_{20}$ = Hypersthene

100% (Hypesthene) = **55%(Enstatite)** + **45%** (**Ferrosilite**) as shown in Table 10a, above.

b. **$(Mg_6Fe_5)Si_{30}O_{71}$** can be converted to real value of Pyroxene Mineral using Binomial Expansion of $Mg_{2-p}Fe_pSiO_4$
Olivine can be arranged in three different ways from more basic to more acidic within its stability field with respect to Gibbs free energy (ΔG) as shown in Figures (19, 20 and 21), below:

$[Mg+iFe]_2 Si_2 O_6 = Mg_2 Si_2 O_6 + i[Mg\,Fe]Si_2 O_6 + i[MgFe]Si_2 O_6 + Fe_2 Si_2 O_6$

$\{Mg_{2-p}Fe_pSi_2O_6\}_{10} = (Mg_{11}Fe_9)(SiO_3)_{20}$

$\{[Mg+iFe]_2 Si_2 O_6\}_{10} = Mg_{10} Si_{20} O_{60} + i[Mg_{10} Fe_{10}]Si_{20} O_{60} + i[Mg_{10} Fe_{10}]Si_{20} O_{60} + Fe_{10} Si_{20} O_{60}$

$Mg_{10}Fe_{10}Si_{20}O_{60} = Mg_{11}Fe_9Si_{20}O_{60}$ $Mg_{10}Fe_{10}Si_{20}O_{60} = Mg_9Fe_{11}Si_{20}O_{60}$

$[Mg+iFe]_{20} Si_{20} O_{60} = Mg_{20} Si_{20} O_{60} + i[Mg_{11} Fe_9]Si_{20} O_{60} + i[Mg_9 Fe_{11}]Si_{20} O_{60} + Fe_{20} Si_{20} O_{60}$

$Mg_{11}Fe_9Si_{20}O_{60}$ = Hypersthene $Mg_9Fe_{11}Si_{20}O_{60}$ = Hypersthene

Olivine can also be arranged in four different ways within its stability field from more basic to more acidic, with respect to Gibbs free energy.

$$\sum_{p=0}^{2}\binom{2}{0}[Mg+iFe]_{n+p} Si_{20}O_{60} = Enstatite$$

$i[\boldsymbol{Mg-Hypersthene}]+i[\boldsymbol{Fe-Hypersth}ene]+Fayalite$

Table 7 above, represents the chemical compositions of Oxides of Pyroxene of KIA1 as analyzed using ICP-MS and can be mathematically analyzed using empiric al formula based on percentage of Calcium Oxide in Kassa Basalt below:

CaO = 10.91%, **MgO = 9.12%, FeO = 13.17%**

Therefore, the chemical compositions of mafic oxides in Pyroxene can be expressed using empirical formula as shown Table 8 below.

Table 8. Empirical Formula for the Mafic Mineral Oxides in KIA1

Oxides of the mineral	MgO	FeO	CaO	SiO_2
% composition of the Oxides	**9.12**	13.17	**10.91**	**66.80**
Molar mass of the Oxides	**40**	**68**	**56**	**60**
$\frac{\%composition}{Molar\ mass}$	$\frac{9.12}{40}$	$\frac{13.17}{68}$	$\frac{10.91}{56}$	$\frac{66.80}{60}$
Ratio of the Oxides	**0.228**	**0.194**	**0.195**	**1.113**
Divide by the smallest number	$\frac{0.228}{0.194}$	$\frac{0.194}{0.194}$	$\frac{0.195}{0.194}$	$\frac{1.113}{0.194}$
	1.18	**1**	**1**	**5.7**
	6	**5**	**5**	**28**
	$(MgO)_6$	$(FeO)_5$	$(CaO)_5$	$(SiO_2)_{28}$
	Mg_6O_6	Fe_5O_5	Ca_5O_5	$Si_{28}O_{56}$
Empirical formula of the Oxides	$(Mg_6Fe_5Ca_5)O_{16}$		$Si_{28}O_{56}$	
Chemical formula of the mineral	$(Mg_6Fe_5Ca_5)Si_{28}O_{72}$			
Mineral 1	**Calcic- Olivine**			
Mineral 1 + SiO_2	$(Mg_6Fe_5Ca_5)Si_{29}O_{74}$			
Mineral 2	**Calcic- Pyroxene**			

a. $(Ca_5Mg_6Fe_5)Si_{29}O_{74}$ can be converted to true value of calcic -Pyroxene Mineral using Zero polynomial of $Mg_{2-p}Fe_pSi_2O_6$

Therefore:

From,

$\Upsilon[Z_0(\beta, \alpha)] = \Upsilon[Z_0(\beta + \alpha)]$

$[Ca(Mg+Fe)\eta]Si_{20}O_{60}$ = $\mathbf{(Ca_5Mg_6Fe_5)Si_{30}O_{71}}$

$\mathbf{(Ca_{0.6}Mg_{0.8}Fe_{0.6})Si_2O_6}$ = $[(Ca_5Mg_6Fe_5)]$ $\mathbf{Si_{29}O_{74}}$

$\mathbf{(Ca_6Mg_8Fe_6)Si_2O_6}$ = $[(Ca_5Mg_6Fe_5)]$ $\mathbf{Si_{29}O_{74}}$

$\mathbf{(Ca_6Mg_8Fe_6)Si_{20}O_{60}}$ = $[(Ca_3Mg_4Fe_3)]$ $\mathbf{Si_{10}O_{30}}$

$\mathbf{(Ca_5Mg_6Fe_5)Si_{29}O_{74}}$ = $[(Ca_3Mg_4Fe_3)]$ $\mathbf{Si_{10}O_{30}}$

$[Ca(Mg+Fe)\eta]Si_{20}O_{60}$ = $[(Ca_3Mg_4Fe_3)]$ $\mathbf{Si_{10}O_{30}}$

$[(Ca_3Mg_4Fe_3)]$ $\mathbf{Si_{10}O_{30}}$ = Calcic-Pyroxene

: $[(Ca_3Mg_4Fe_3)]$ $\mathbf{Si_{10}O_{30}}$ {**CaO = 30%, MgO = 40%, FeO = 30%**}

Therefore:

Fore, **Ca = 30% (20%<Ca<45%)**
Mg: Fe = 70%
Mg = 40%, Fe = 30%u
$[Mg_{40}: Fe_{30}]$ = 70%
$Ca_{30}[(MgFe)_{70}$ = 100%
Then,
From $\Upsilon[Z_0(\beta, \alpha)] = \Upsilon[Z_0(\beta + \alpha)]$

$[\Upsilon(\beta + \alpha)]Z_p = [(\Upsilon, \beta)]Z_p + [(\Upsilon, \alpha)]Z_p$
Then,
$[\Upsilon(\beta + \alpha)]Z_p \sim 100\%$
$[\Upsilon_{30}(\beta + \alpha)_{70}]Z_p = [(\Upsilon_{30}, \beta_{40})]Z_p + [(\Upsilon_{30}, \alpha_{30})]Z_p$
$Ca_{30}[(Mg_{40}: Fe_{30})]Z_p = Ca_{30}[(Mg_{40} + Fe_{30})]Z_p$
$Z_p = Si_{10}O_{30}$
$[Ca_{30}(Mg+Fe)_{35}]Si_{20}O_{60} = [(Ca_{30}Mg_{40})]Si_{100}O_{300} + [(Ca_{30}Fe_{30})]Si_{100}O_{300}$
$[Ca_{30}(Mg+Fe)_{35}]Si_{100}O_{300}=[(Ca_{30}Mg_{70})]Si_{100}O_{300}+[(Ca_{30}Fe_{30}Mg_{40})]Si_{100}O_{300}+[(Ca_{30}Fe_{40}Mg_{30})]Si_{100}O_{300}+[(Ca_{30}Fe_{70})]Si_{100}O_{300}$
AUGITE SERIES = $[(Ca_{30}Fe_{30}Mg_{40})]Si_{100}O_{300}$
AUGITE SERIES = 17% <u>$[(Ca_3Fe_3Mg_4)]Si_{10}O_{30}$</u>
Magnesio-Augite = $[(Ca_3Mg_7)]Si_{10}O_{30}$
Ferro-Augite = $[(Ca_3Fe_7)]Si_{10}O_{30}$
$(Wo_3En_4Fe_3)$ = 10

$Wo_{30}\ En_{40}.Fe_{30}$ = 100%

100% (Augite) = **30%(Wollastonte)** + 40%(**Enstatite**) + **30%** (**Ferrosilite**) as shown in Table 10a, above.

Therefore, For 17%(Augite)

17% (Augite) = **5.1%(Wollastonite)** + 6.8%(**Enstatite**) + **3.6%** (**Fayalite**) **of KIA1** in **Kassa Volcanic Field**

B: Classification of Mafic Pyroxene of KIA1 in Kassa Volcanic Field.

➢**Pyroxene classes** = 1[basic '**Pyroxene**'] + [intermediate '**Pyroxene**'] + i[acidic **Pyroxene**].
➢**Pyroxene classes** = 1[basic '**Enstatite**'] + [intermediate '**Hypersthene**'] + i[acidic **Ferrosilite**].
➢**Pyroxene Minerals** = [basic'**Augite**']+ i[intermediate'**Augite**'] + i[intermediate'**Augite**'] +[acidic '**Augite**']
['**augite** '] = ['**Calcic-pyroxene**']
['**KIA1** '] = ['**Augite**']
['**KIA1** '] = ['**Calci-pyroxene**']
$Mg_{2-p}Fe_pSi_2O_6$ is a **'Pyroxene series'** formula that can be used to calculate all Pyroxene minerals from the melt $\mathfrak{W}$, where p is an integer and ranges from 0 to 2 in Pyroxene crystals. At certain value of p, Hypersthene and Augite crystallize depending on their stability fields with chemical formula of **$(Mg_6Fe_5)Si_{30}O_{71}$** and **$[(Ca_3Fe_3Mg_4)]Si_{10}O_{30}$**. Therefore (**17%**) of **Augite** is the primary calcic - Pyroxene in the mafic olivine series of Kassa Volcanic Field.\

4.4.3 Empirical formula and classifications for Felsic Oxides of KIA1 in Kassa Volcanic Field using Zero Polynomial of $\left(Q_{4-y}N_y\right)W_i$

Table 4 above, represents the chemical compositions of Oxides of felsic mineral of KIA1 as analyzed using ICP-MS and can be mathematically analyzed using empirical formula below:

A: **Empirical Formula for Felsic Oxides of KIA1**

Therefore, the volume percent of Felsic Oxides of KIA1 are:

CaO = **8.50%** in KIA1

Al_2O_3 = **14.23%** in KIA1

Na_2O = **4.47%** in KIA1

SiO_2 = **52.0%** in KIA1

8.5% + 14.23% +4.47+ 52.0% = 79.20%

The Total volume percent of Felsic Oxides of KIA1 = 74.73%

CaO% + Na_2O+ Al_2O_3% + SiO_2 % = Plagioclase %

CaO = **10.73%** in Plagioclase

Al_2O_3 = **17.97%** in Plagioclase

Na_2O = **5.64%** in Plagioclase

SiO_2 = **65.66%** in Olivine

Therefore, the chemical compositions of felsic oxides in Olivine can be expressed using empirical formula as shown Table 9 below.

Table 9. Empirical Formula for the Felsic Oxides in KIA1

Oxides of the mineral	**CaO**	**Na_2O**	**Al_2O_3**	**SiO_2**
% composition of the Oxides	**10.73**	5.64	**17.97**	**65.66**
Molar mass of the Oxides	**56**	**62**	**100**	**60**
$\frac{\%composition}{Molar\ mass}$	$\frac{10.7\ 3}{56}$	$\frac{5.64}{62}$	$\frac{17.97}{100}$	$\frac{65.66}{60}$
Ratio of the Oxides	**0.192**	**0.091**	**0.180**	**1.094**
Divide by the smallest number	$\frac{0.192}{0.091}$	$\frac{0.091}{0.091}$	$\frac{0.180}{0.091}$	$\frac{1.094}{0.091}$
	2.11	**1**	**1.98**	**12.02**
	2	**1**	**2**	**12**
	$(CaO)_2$	**(Na_2O)**	**$(Al_2O_3)_2$**	**$(SiO_2)_{12}$**
	Ca_2O_2	**Na_2O_1**	**Al_4O_6**	**$Si_{12}O_{24}$**
Emprical formula of the Oxides	**$(Ca_2Na_2)O_3$**		**Al_4O_6**	**$Si_{12}O_{24}$**
Chemical formula of the mineral	**$(CaNa)_2\ (Al_4\ Si_{12})\ O_{33}$**			
Mineral 1	**Plagioclase feldspar**			
Mineral 1 + SiO_2				
Mineral 2				

$(CaNa)_2(Al_4Si_{12})O_{33}$ cannot be convertible using Zero polynomial of because there is no polymerization in feldspar.

Therefore using empirical formula, is **$(CaNa)_2(Al_4Si_{12})O_{33}$**, as shown in Table 24 above.

Then the true value of Plagioclase feldspar Mineral using Zero polynomial of $(Q_{4-y}N_y)W_i$ is **$(CaNa)_2(Al_4Si_{12})O_{33}$**

The roots (λ η) and (λᵧ) of **= $(CaNa)_2(Al_4Si_{12})O_{33}$** are {2, 2} and {4, 12} respectively and the solution = **$(CaNa)_2(Al_4Si_{12})O_{33}$**

$(CaNa)_2(Al_4Si_{12})O_{33}$ = 47% Andesine

$An_{50}.Ab_{50}$ = 100%

100% (Andesine) = **50%(Anorthite)** + **50%** (**Albite**) as shown in Table 20a, above.

Therefore, For 47%(Andesine)

$(Fo(\frac{50x47}{100})\ Fa(\frac{50x47}{100}))\% = An_{23.5}.Ab_{23.5}$

47% (Andesine) = **23.5%(Forsterite)** + **23.5%** (**Fayalite**) **of KIA1** in **Kassa Volcanic Field**

B: Classification of Felsic Minerals of KIA1 in Kassa Volcanic Field.

➢**Feldspar classes** = 1[basic'**Feldspar**'] + [intermediate'**Feldspar**'] + i[acidic **Feldspar**].
➢**Feldspar Minerals** = [basic'**Anorthite**'] + i[intermediate'**Andesine**'] + i[intermediate'**Andesine**'] +[acidic '**Albite**']
['**Andsine** '] = ['**intermediate Feldspar**']
['**KIA1** '] = **47%**['**Andesine**']
['**KIA1** '] = ['**intermediate Feldspar**']

4.4.4 Empirical formula and classifications for Ferrous/Ferric Oxides of Iron Ore of KIA1 in Kassa Volcanic Field using Zero Polynomial of $(\beta_{3-p}\ \alpha_p)(Z_0)_{\bar{i}}$

Table 4 above, represents the chemical compositions of **Ferrous/Ferric** Oxide of KIA1 as analyzed using ICP-MS and can be mathematically analyzed using empirical formula below:

A: Emperical Formula for the Ferrous/Ferric Oxides of Iron Ore of KIA1

Therefore, the volume percent of Ferrous Oxides in KIA1 are:

FeO = **10.25%** in KIA1

TiO_2 = **2.26%** in KIA1

10.25% + 2.26% = 12.51%

The Total volume percent of Ferrous Oxides in KIA1 = 12.51%

FeO = **81.93%** in Iron Ore

TiO_2 = **18.07%** in Iron Ore

Therefore, the chemical compositions of Ferrous oxides in Iron ore can be expressed using empirical formula as shown Table 10 below.

Table 10. Empirical Formula for the Ferrous Oxides of KIA1

Oxides of the mineral	**FeO**	**TiO_2**
% composition of the Oxides	**81.93**	18.07
Molar mass of the Oxides	**68**	**78**
$\frac{\%composition}{Molar\ mass}$	$\frac{81.93}{68}$	$\frac{18.07}{78}$
Ratio of the Oxides	**1.20**	**0.23**
Divide by the smallest number	$\frac{1.20}{0.23}$	$\frac{0.23}{0.23}$
	5.2	**1**
	5	**1**
	$(FeO)_5$	**(TiO_2)**
	Fe_5O_5	**TiO_2**
Emprical formula of the Oxides	**$(Fe_5Ti)O_7$**	
Chemical formula of the mineral	**$(Fe_5Ti)O_7$**	
Mineral 1	**Ferrous Iron ore**	
Mineral 1 + TiO_2	**$(Fe_5Ti_2)O_9$**	
Mineral 2	**Ferric Iron ore**	

a. Conversion of **$(Fe_5Ti)O_7$** to true value of Iron ore Mineral using Zero polynomial of $Fe_{3-p}Ti_pO_4$
Therefore:

$Fe_{3-p}Ti_pO_4$ **= $(Fe_5Ti)O_7$**

$(Fe_2Ti)O_4$ = $(Fe_5Ti)O_8$

The roots ($\lambda\,\eta$) of $Fe_{2-p}Ti_pO_4$ **= $(Fe_5Ti)O_8$** are 5 and 1 respectively and The solution = $(Fe_2Ti)O_4$

$Fe_{83}Ti_{17}$ = 100%

100% (<u>Ulvospinel)</u> = **83%(<u>Wustite)</u>** + **17%** (**<u>Rutile</u>**).

Therefore, For 7%(<u>Ulvospinel)</u>

$(Fo(\frac{83x7}{100})\,Fa(\frac{17x7}{100})\% = (FeO)_6\,(TiO_2)_1$

8% (<u>Ulvospinel)</u> = **7%(<u>Wustite)</u>** + **1%** (**<u>Rutile</u>**) **of KIA1** in **Kassa Volcanic Field**

For ferric oxide:

$Fe_{2-p}Ti_pO_3$ **= $(Fe_5Ti_2)O_9$**

$(FeTi)O_3$ = $(Fe_{14}Ti_6)O_{30}$

$(Fe_{14}Ti_6)O_{30}$ = Ilmenite

The roots ($\lambda\,\eta$) of $Fe_{2-p}Ti_pO_3$ **= $(Fe_5Ti_2)O_9$** are 14 and 6 respectively and

The solution = **$(Fe_{14}Ti_6)O_{30}$**

$(FeO)_{71}\,(TiO_2)_{29}$ = 100%

100% (<u>Ulvospinel)</u> = **71%(<u>Wustite)</u>** + **29%** (**<u>Rutile</u>**).

Therefore, For 7%(<u>Ilmenite)</u>

7% (<u>Ilmenite)</u> = **5%(<u>Wustite)</u>** + **2%** (**<u>Rutile</u>**) **of KIA1** in **Kassa Volcanic Field**

B: Classification of Iron Ore Minerals of <u>KIA1</u> in Kassa Volcanic Field<u>.</u>

➢**Iron Ore classes** = 1[basic'**<u>Iron Ore</u>**'] + [intermediate'**<u>Iron Ore</u>**'] + i[acidic **<u>Iron Ore</u>**].
➢**Iron Ore Minerals** = ['basic **<u>Magnetite</u>**'] + i[Titano-manetite'] + i[Titano-magnetite'] +[acidic'**<u>Ulvospinel</u>**']
➢**Iron Ore Minerals** = ['basic **<u>Haematite</u>**'] + i[Titano-manetite'] + i[Titano-magnetite'] +[acidic'**<u>Ilmenite</u>**']
['**<u>Ulvospinel</u>**'] = ['**<u>acidic Iron Ore</u>**']
['**<u>KIA1</u>**'] = **7%** ['**<u>Ulvospinel</u>**']
['**<u>KIA1</u>**'] = ['**<u>acidic Iron Ore</u>**']

Table 11. Mineralogical Compositions and Rock type of KIA1 in Kassa Volcanic Field

Minerals	Olivine	Pyroxene	Feldspar	Iron ore	Silica	Others
Chemical formula	**$Mg_{11}Fe_9(Si_1O_4)_{10}$**	**$[(Ca_3Fe_3Mg_4)](Si_1O_3)_{10}$**	**$(CaNa)_2(Al_4Si_{12})O_{33}$**	**$(Fe_2Ti)(O_4)$**	SiO_2	
Mineral type	Hyalosiderite	Augite	Andesine	Ulvospinel	Quartz	
Percentage (%)	8	17	47	7	0	21
Alkali content	Na_2O+K_2O = **4.47%** Na_2O+K_2O > **3%**					
Rock type	Alkaline Oivine Basalt, **Gabbro, ⇒ Olivine 5%**					

(a) Mathematrical Observations of the **Rock of KIA1 in Kassa Volcanic Field:**

Mathematically, the Mineralogical compositions of the Rock of **KIA1 are**,

➢**<u>8% Hyalosiderite</u>** of olivine,
➢**<u>17% Augite</u>** of pyroxene,
➢**<u>47% Andesine</u>** of plagioclase
➢**<u>7% Ulvospinel</u>** of iron ore,
➢0% **<u>Quartz</u>.**

(b) Mathematical analysis of the <u>KIA1 Slide</u> in Kassa Volcanic Field as presented in the pictures below.

1. Porphyritic texture
20% porphyritic consisting:

- **<u>Augite</u>** (**5%**)
- **<u>Hyalosiderite</u>** (**8%**)
- **<u>Andesine</u>** (7%).

3.Groundmass

77% groundmass (neglecting vesicles) consisting

- **40% <u>Andesine</u>** which is euhedral to subhedral shaped
- **12% <u>Augite</u>** which is subhedral to anhedral
- **7% <u>Ulvospinel</u>**, which exhibits anhedral enlogate shape (**ilmenite**?)

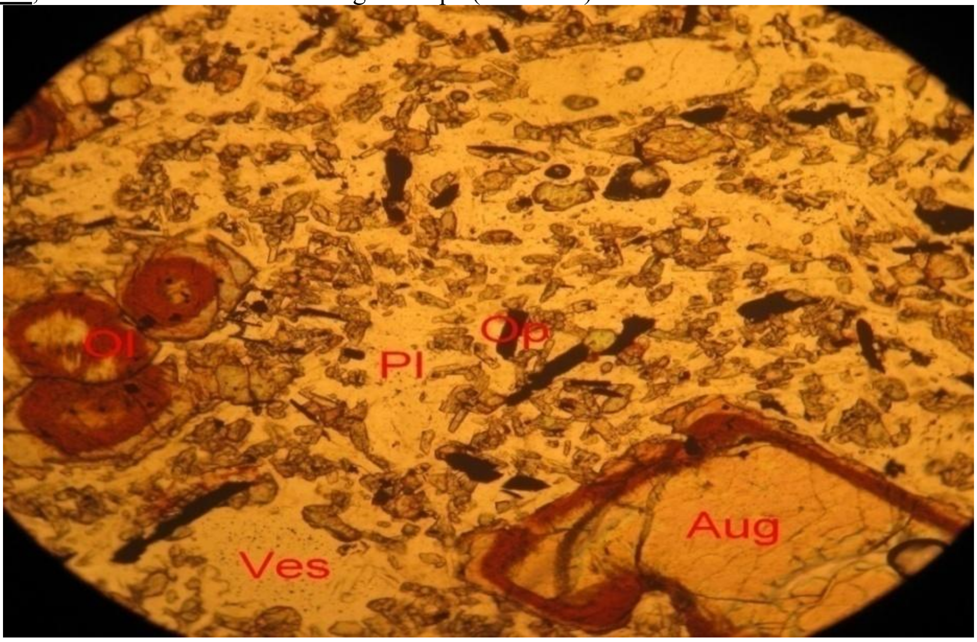

Photomicrograph of KIA 1, PPL showing the 8% of <u>Hyalosiderite</u> and 17% of <u>Augite</u> rounded by rims (pigeonite?), 47% of <u>Andesine</u> and 7% of <u>Ulvospinel</u>

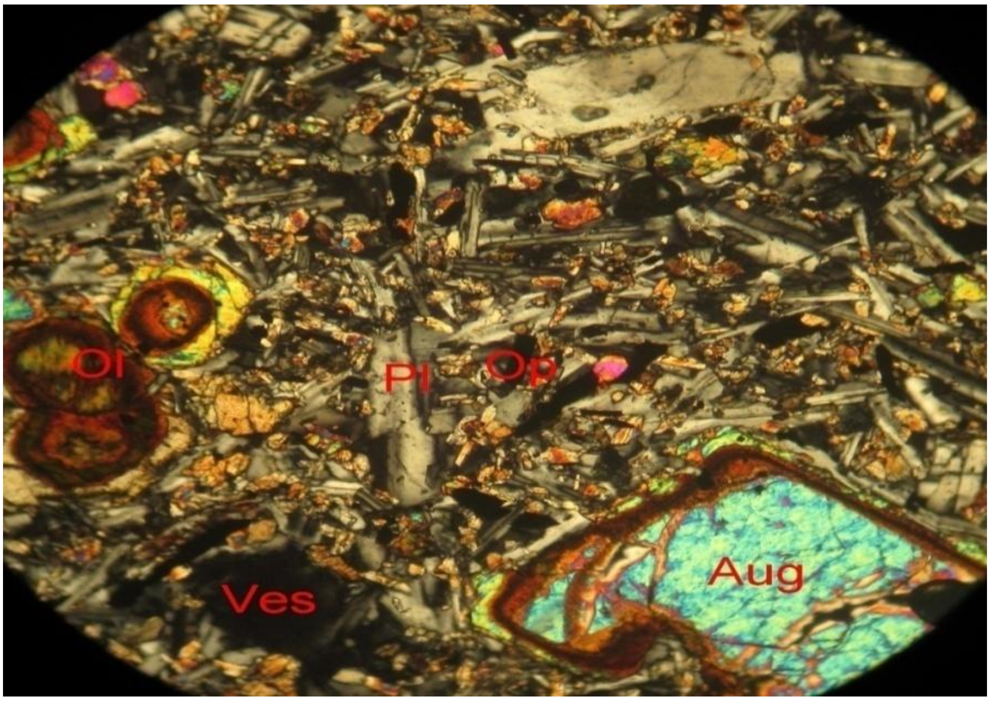

Photomicrograph of KIA1, XPL showing 8% of **<u>Hyalosiderite</u>** and **17%** of **<u>Augite</u>** rounded by rims (**pigeonite**?), **47%** of **<u>Andesine</u>** and **7%** of **<u>Ulvospinel</u>**

(c) Using Metrical Matrices:

<u>1. Metrical Matrix for Mafic Olivine Minerals and Feldspars:</u>

$$\begin{bmatrix} Anorthite \\ Forsterite \end{bmatrix} + \begin{bmatrix} Albite \\ Fayalite \end{bmatrix} = \begin{bmatrix} Andesine \\ Hyalosiderite \end{bmatrix}$$

$\begin{bmatrix} Andesine \\ Hyalosiderite \end{bmatrix}$ = [**Alkali Olivine Basalt**]

2. <u>Metrical Matrix for Mafic Pyroxene Mineral and Feldspar</u>:

$\begin{bmatrix} Andesine \\ Hyalosiderite \end{bmatrix}$+ [**Alkali Olivine Basalt**]

3. <u>Metrical Matrix for Augite Pyroxene Mineral and Feldspar</u>:

+ $\begin{bmatrix} Andesine \\ Augite \end{bmatrix}$= [**<u>Alkali Olivine Basalt</u>]**

With total alkali greater than **3%** (Na_2O + k_2O >**3%**), and the modal olivine greater **5%**, the expected basic rocks classification depending on their grain sizes, are **<u>alkaline olivine gabbro</u>**, **<u>alkaline Olivine dolerite</u>, <u>alkaline Olivine norite</u> or <u>alkaline olivine basalt</u>** as presented in the picture below:

Alkaline Olivine basalt at Kassa with total alkaline content greater than 3% and modal olivine greater than 5%.

5. Summary and Conclusion

5.1 Summary of Findings

In summary, the mathematical equations were used to calculate minerals in Basalts and as it outlines below:

1. Zo is the nucleation point of the recharged magma under thermodynamic condition and it is the silicate identity in the magma which is the building block of silicate minerals.

2. is the “formula” to calculate Mafic minerals from the magma under thermodynamic change

3. (is the formula to calculate for complex minerals under thermodynamic change, where (is the lattice of ions of different sizes and charges and is another lattice of ions of different sizes and charges in the same mineral to maintain electrical neutrality in the minerals

4. Applying these formulae from number 1 and 2, it results to matrices to produce the resultant rocks as given bellow:

If P > A, then the intermediate rock is the Andesite

[Basalt] + [Dacite] = Andesite

P < A, then the intermediate rock is the trachyte

[Basalt] + [Rhyolite] = Trachyte

If P = A, then the intermediate rock is the Hybrid Monzonite

[Basalt] + [Rhyolite] = Hybrid Monzonite

5. Using petrographic microscope, minerals observed during studies of Kassa basalts are mathematically represented by

Matrix Method: the minerals that set in matrix include, olivine, pyroxene and plagioclase

Set Notation: they are the elements that form set when partitioned in Kassa Basalts. They include [Cr, Zr, Ni, Mn, Sr, Va and Ba]

6. The mathematical analysis after extensive geochemical analysis and petrographic studies indicates that Kassa Basalts are

Olivine Basalt: Olivine > 5%,

: Na2O < 3%

Alkali Olivine Basalt: Olivine > 5%,

: Na2O >3%

Tholeiite Basalt type : Olivine > 5%,

: Na2O >3%

5.2 Conclusion

Using Bowen's and Goldschmidt concepts according Achuenu and others (2025), the formula for mafic minerals and (for felsic and complex minerals were successfully used in this research to calculate the numerical values of minerals in Kassa basalt, particularly, For KIA1.

From the Mathematical modeling, it is also concluded, that the examinations of sampled rocks collected from Kassa Volcanic Basalts, under thin section, chemical analysis using ICPMS, and mathematical computation indicate, that minerals observed and chemical composition analyzed, fall within gabbro clan [18]. The gabbro clan includes basalt, dolerite, norite, scoria and gabbro. The minerals observed in these rocks under thin section are restricted to Gabbro clan and they are mainly basic, because of its instability in the presence of free silica. It is on this note, conclusion was made that, mathematically Kassa volcanic Basalts particularly for KIA1 as shown in Table 3 and 4 above, are characteristics of rocks of Gabbro clan and the rock type for KIA1 is olivine, alkali basalt magma type as shown in Table 3 and 4 above.

References

[1] Achuenu I., Lekmang.C.I.,Hyeladi.D,. And Geoffry M.K., (2025). Mathematical Modeling of Goldschmidt and Bowen's Crystallization of Mafic Magma: Implication for the Crystallization of Basaltic Rocks. Global educational Research: 2360-7963 Vol. 13(4) May, Pp. 141-158, 2025

[2] Goldschmidt, V. M., 1926, Geochemische Verteilungsyesetze der Elemente VII. Die Gesetze der Kristallochemie, Skrfler Norske Videnskaps-Akad. Oslo,'I, Mat. Naturv. Kl, 2,5-116.

[3] [54] Ringwood, A.E. 1962. A Model for the Upper Mantle. J. Geophys. Res. 67, 4473 - 4477.

[4] Barth, K. (1962). Theological Dialogue. Theology Today, 19(2), 171-177. https://doi.org/10.1177/004057366201900204

[5] Mendele'ev D. (1877). Entstehungund Vorkommen des materials Dtsch. Chem.Gas. Ber: 10, 229.

[6] Green, D. H., and Ringwood, A. E. (1969). The Origin of basalt magma, Amer. Geophys Union mongr., 489-94.

[7] Nackolds, S. R., 1966, The behavior of some elements during fractional crystallization of v/ magma, Geochim. Cosmochim. Acta, 30, 267-278.

[8] Fournier, R.O., and Potter, R.W. 11, (1992a): An equation equation correlating the solubility of quartz in water from 250C to 9000C at Chim. Acta, 46, 1969 – 1974.

[9] Wager, L.R. and Brown, G.M. 1967. Layered Igenous Rocks, Freeman, San Francisco.

[10] Atsushi Toramaru, & Tsuyoshi Kichise. (2023). A New Model of Crystallization in Magmas: Impact of Pre-Exponential Factor of Crystal Nucleation Rate on Cooling Rate Exponent and Log-Linear Crystal Size Distribution. Journal of Geophysical Research Solid Earth, 128(10). https://doi.org/10.1029/2023jb026481

[11] McBirney, A. R., and H. Williams, 1969, Geology and Petrology of the Galapagos Islands, Ceol. Soc. America Mem. 118,197p.

[12] Kuno, H., 1968, Differentiation of Basalt Magmas, in The Poldervaart Treatise on Rocks of Basaltic Composition, vol. 2, Basalts, H. H. Hess and A. Poldervaart, eds., Wiley-lnterscience, New York, pp. 623-688.

[13] Kuno, H.I. 1960. High-Alumina Basalts. J. Petrol. I, 121 -141.

[14] Kushiro, I., and H. Kuno, 1963, Origin of Primary Basalt Magmas and Classification of Basaltic Rocks, lour. Petrology4:75-89.

[15] Mendele'ev D. (1902). The principle of chemistry, 2nd English ed: Vol.1, (Translated from 6th Russian ed:) Collier, New York.

[16] Bujns, R. G., Clark, R. H.«and Fyfe, W. S., 1964, Crystal-field theory and application to / problems in geochemistry, in Chemistry of the Earth's Crust, Vemadsky Centennial Symposium. Vol. 2 (Vinogradov, ed.), Moscow, pp. 88-106.

[17] Yoder, H. S. and Tilley, E.C. 1962. Origin of Basaltic Magmas: An Experimental Study of Natural and Synthetic Rock Systems. J. Petrol. 3, 342 - 532.

[18] Ahrens, i. H., 1965, Distribution of the Elements in Our Planet, McGraw-Hill, New York, llOjip.: "6old, T: and Soter, S. (1982).